

ปฏิกริยาดีไฮโดรจีเนชันของเอทานอลเป็นอะซีตัลดีไฮด์บนตัวเร่งปฏิกริยาถ่านกัมมันต์



นางสาวสมฤดี ชัชวาลรัตน์

จุฬาลงกรณ์มหาวิทยาลัย

CHULALONGKORN UNIVERSITY

วิทยานิพนธ์นี้เป็นส่วนหนึ่งของการศึกษาตามหลักสูตรปริญญาวิศวกรรมศาสตรมหาบัณฑิต

สาขาวิชาวิศวกรรมเคมี ภาควิชาวิศวกรรมเคมี

คณะวิศวกรรมศาสตร์ จุฬาลงกรณ์มหาวิทยาลัย

ปีการศึกษา 2556

ลิขสิทธิ์ของจุฬาลงกรณ์มหาวิทยาลัย

บทคัดย่อและแฟ้มข้อมูลฉบับเต็มของวิทยานิพนธ์ตั้งแต่ปีการศึกษา 2554 ที่ให้บริการในคลังปัญญาจุฬาฯ (CUIR)

เป็นแฟ้มข้อมูลของนิสิตเจ้าของวิทยานิพนธ์ ที่ส่งผ่านทางบัณฑิตวิทยาลัย

The abstract and full text of theses from the academic year 2011 in Chulalongkorn University Intellectual Repository (CUIR) are the thesis authors' files submitted through the University Graduate School.

DEHYDROGENATION OF ETHANOL TO ACETALDEHYDE OVER ACTIVATED CARBON  
CATALYSTS

Miss Somrudee Chatchawanrat



จุฬาลงกรณ์มหาวิทยาลัย

CHULALONGKORN UNIVERSITY

A Thesis Submitted in Partial Fulfillment of the Requirements  
for the Degree of Master of Engineering Program in Chemical Engineering

Department of Chemical Engineering

Faculty of Engineering

Chulalongkorn University

Academic Year 2013

Copyright of Chulalongkorn University

Thesis Title	DEHYDROGENATION OF ETHANOL TO ACETALDEHYDE OVER ACTIVATED CARBON CATALYSTS
By	Miss Somrudee Chatchawanrat
Field of Study	Chemical Engineering
Thesis Advisor	Associate Professor Bunjerd Jongsomjit, Ph.D.

---

Accepted by the Faculty of Engineering, Chulalongkorn University in Partial  
Fulfillment of the Requirements for the Master's Degree

.....Dean of the Faculty of Engineering  
(Professor Bundhit Eua-arporn, Ph.D.)

THESIS COMMITTEE

.....Chairman  
(Assistant Professor Suphot Phatanasri, D.Eng.)

.....Thesis Advisor  
(Associate Professor Bunjerd Jongsomjit, Ph.D.)

.....Examiner  
(Chutimon Satirapipathkul, D.Eng.)

.....External Examiner  
(Ekrachan Chaichana, D.Eng.)

สมฤดี ชัชวาลรัตน์ : ปฏิกริยาดีไฮโดรจีเนชันของเอทานอลเป็นอะซีตัลดีไฮด์บนตัวเร่ง  
ปฏิกริยาถ่านกัมมันต์. (DEHYDROGENATION OF ETHANOL TO ACETALDEHYDE  
OVER ACTIVATED CARBON CATALYSTS) อ.ที่ปรึกษาวิทยานิพนธ์หลัก: รศ. ดร.  
บรรเจิด จงสมจิตร, 69 หน้า.

งานวิจัยนี้มุ่งศึกษาเกี่ยวกับคุณสมบัติและความว่องไวของถ่านกัมมันต์ที่ได้จากกากรำ  
ข้าวโดยใช้วิธีการกระตุ้นทางเคมีด้วยซิงค์คลอไรด์ที่อุณหภูมิในการกระตุ้นแตกต่างกันเพื่อเป็น  
ตัวเร่งปฏิกริยาสำหรับเอทานอลดีไฮโดรจีเนชัน จากการศึกษาพบว่า ถ่านกัมมันต์ที่ได้จากกากรำ  
ข้าวแสดงทั้งลักษณะโครงสร้างรูพรุนแบบไมโครพอร์และมีโซพอร์ ถ่านกัมมันต์ที่ได้จากกากรำข้าว  
เหล่านี้แสดงหน้าที่หลักในการเป็นตัวเร่งปฏิกริยาเอทานอลดีไฮโดรจีเนชันซึ่งผลิตอะซีตัลดีไฮด์เป็น  
ผลิตภัณฑ์หลัก อาจจะเนื่องมาจากซิงค์ที่ตกค้างจากระบวนการเตรียมถ่านกัมมันต์ นอกจากนี้  
ยังเน้นศึกษาถึงการใช้ถ่านกัมมันต์(ทางการค้า)เป็นตัวรองรับตัวเร่งปฏิกริยานิกเกิลสำหรับเอทา  
นอลดีไฮโดรจีเนชันด้วย พบว่าการกระจายตัวของนิกเกิลบนถ่านกัมมันต์ชนิดทางการค้ามีลักษณะ  
ที่ดี ซึ่งการเติมนิกเกิลไปยังถ่านกัมมันต์จะเพิ่มความว่องไวในการเร่งปฏิกริยาสำหรับเอทานอลดี  
ไฮโดรจีเนชันเกิดเป็นอะซีตัลดีไฮด์ นอกจากนี้ ตัวเร่งปฏิกริยานิกเกิลที่ถูกรองรับด้วยถ่านกัมมันต์  
ชนิดทางการค้าแสดงร้อยละการเปลี่ยนแปลงเอทานอลสูงกว่าตัวเร่งปฏิกริยานิกเกิลที่ถูกรองรับ  
ด้วยถ่านกัมมันต์ที่ได้จากกากรำข้าว ทั้งนี้อาจเนื่องมาจากการรวมตัวกันของนิกเกิลกลายเป็นผลึก  
ขนาดใหญ่

จุฬาลงกรณ์มหาวิทยาลัย  
CHULALONGKORN UNIVERSITY

ภาควิชา วิศวกรรมเคมี

สาขาวิชา วิศวกรรมเคมี

ปีการศึกษา 2556

ลายมือชื่อนิสิต .....

ลายมือชื่อ อ.ที่ปรึกษาวิทยานิพนธ์หลัก .....

# # 5570409421 : MAJOR CHEMICAL ENGINEERING

KEYWORDS: ETHANOL DEHYDROGENATION / ACTIVATED CARBON / NICKEL  
CATALYST / ACETALDEHYDE PRODUCTION

SOMRUDEE CHATCHAWANRAT: DEHYDROGENATION OF ETHANOL TO  
ACETALDEHYDE OVER ACTIVATED CARBON CATALYSTS. ADVISOR: ASSOC.  
PROF. BUNJERD JONGSOMJIT, Ph.D., 69 pp.

This research focused on investigation of the characteristic and catalytic activity of activated carbon derived deoiled rice bran using chemical activation with zinc chloride by various activation temperatures as catalyst for the ethanol dehydrogenation. It was found that activated carbons derived deoiled rice bran are presented of both microporous and mesoporous. These activated carbons derived deoiled rice bran act mainly as ethanol dehydrogenation catalyst which produced acetaldehyde as the main product, probably due to presence of zinc residue from preparation activated carbon. Furthermore, activated carbon (commercial grade) used as catalyst support for nickel catalyst on the ethanol dehydrogenation was also investigated. It was found that nickel distribution on the commercial activated carbon was good. Loading nickel onto activated carbon increases the catalytic activity for ethanol dehydrogenation towards acetaldehyde. In addition, nickel catalyst supported on commercial activated carbon showed higher ethanol conversion than nickel catalyst supported on activated carbon derived rice bran, which might be attributed to the aggregation of nickel into large crystalline.

จุฬาลงกรณ์มหาวิทยาลัย  
CHULALONGKORN UNIVERSITY

Department: Chemical Engineering      Student's Signature .....

Field of Study: Chemical Engineering      Advisor's Signature .....

Academic Year: 2013

## ACKNOWLEDGEMENTS

The author would like to express greatest gratitude and appreciation to her advisor, Associate Professor Bunjerd Jongsomjit for the continuous support and enlightening me in all the times of this research, for his invaluable guidance, suggestion, immense knowledge and motivation throughout of this study. Beside her advisor, the author is also grateful to thesis committee: Assistant Professor Suphot Phatanasri, Chutimon Satirapipathkul and Ekrachan Chaichana for insightful comments. The author would like to thank the Thailand Research Fund (TRF).

In addition, the author would like to thank for kind suggestion to Mr.Jakrapan Janlamool and Dr.Mingkwan Wannaborworn. Also the author thanks all my friends and members of the Center of Excellent on Catalysis & Catalytic reaction laboratory for encouragement and assistance. To the others, not specifically named, who help and support on this thesis, please be assured that she thinks of you.

Most of all, the author would like to express her highest gratitude to her parents who always pay attention to her all the times for suggestion, support and encouragement.

## CONTENTS

	Page
THAI ABSTRACT .....	iv
ENGLISH ABSTRACT .....	v
ACKNOWLEDGEMENTS .....	vi
CONTENTS .....	vii
LIST OF FIGURES .....	viii
LIST OF TABLES .....	x
LIST OF SCHEMES .....	xi
CHAPTER 1 INTRODUCTION .....	1
CHAPTER 2 THEORIES.....	4
CHAPTER 3 LITERATURE REVIEWS.....	12
CHAPTER 4 EXPERIMENTAL.....	19
CHAPTER 5 RESULTS AND DISCUSSION .....	27
CHAPTER 6 CONCLUSIONS AND RECOMMENDATIONS.....	57
REFERENCES .....	59
APPENDICES.....	62
APPENDIX A.....	63
APPENDIX B.....	64
APPENDIX C.....	67
VITA.....	68
LIST OF PUBLICATION .....	69

## LIST OF FIGURES

Figure 1.1 Rice seed composition.....	1
Figure 2.1 Structure of oxygen functional group on carbon surfaces.....	7
Figure 2.2 Mechanism for the dehydration of ethanol to ethylene .....	11
Figure 3.1 Proposed the formation partway of ether and ethene form ethanol dehydration on oxidized carbon .....	15
Figure 5.1 N <sub>2</sub> adsorption-desorption isotherms at -196°C of the activated carbon derived deoiled rice bran.....	27
Figure 5.2 XRD patterns of activated carbon catalysts .....	29
Figure 5.3 Thermal analysis of activated carbon derived deoiled rice bran by various activation temperatures .....	31
Figure 5.4 FT IR spectra of activated carbon catalysts .....	33
Figure 5.5 Conversion of ethanol as a function of reaction temperature using activated carbon catalysts .....	35
Figure 5.6 Selectivity of acetaldehyde as a function of reaction temperature using activated carbon catalysts .....	36
Figure 5.7 Yield of acetaldehyde as a function of reaction temperature using activated carbon catalysts .....	37
Figure 5.8 Ethanol conversion and selectivity of products as a function of reaction temperature using AC <sub>c</sub> 400 catalyst .....	38
Figure 5.9 N <sub>2</sub> adsorption-desorption isotherms at -196°C of the nickel catalysts supported on activated carbon .....	40
Figure 5.10 BJH pore size distribution for porous carbon catalysts .....	42
Figure 5.11 XRD patterns of nickel catalysts supported on activated carbon.....	43
Figure 5.12 TEM micrograph of nickel catalysts supported on activated carbon .....	44
Figure 5.13 SEM micrograph of nickel catalysts supported on activated carbon .....	45
Figure 5.14 EDX mapping of nickel catalysts supported on activated carbon .....	46
Figure 5.15 Thermal analysis of AC <sub>c</sub> sample under nitrogen atmosphere .....	48
Figure 5.16 in situ TGA/DTG analysis of activated carbon impregnated with Ni(NO <sub>3</sub> ) <sub>2</sub> · 6H <sub>2</sub> O (without calcination)under air.....	49



Figure 5.17 Proposed decomposition of nickel catalysts during calcination with air... 51	51
Figure 5.18 The deconvolution of Ni 2p of nickel catalysts from XPS analysis ..... 52	52
Figure 5.19 Conversion of ethanol as a function of reaction temperature using nickel catalysts..... 54	54
Figure 5.20 Selectivity of products as a function of reaction temperature using nickel catalysts..... 55	55
Figure D.1 The calibration curve of ethanol ..... 65	65
Figure D.2 The calibration curve of acetaldehyde..... 65	65
Figure D.3 The calibration curve of ethylene ..... 66	66
Figure D.4 The calibration curve of di-ethyl ether..... 66	66

## LIST OF TABLES

Table 2.1 some reaction catalyzed by carbon.....	8
Table 2.2 Physical properties of nickel.....	9
Table 3.1 Main characteristic of different activated carbon at optimum condition.....	12
Table 4.1 Operating condition of gas chromatograph.....	26
Table 5.1 Porous properties of activated carbon from deoiled rice bran.....	28
Table 5.2 Total acid density and amount of impurities of activated carbon.....	32
Table 5.3 The contaminants of a commercial activated carbon obtained by EDX.....	39
Table 5.4 Porous properties of nickel catalysts and commercial activated carbon....	41
Table 5.5 EDX analysis of nickel catalysts supported on activated carbon.....	47
Table 5.6 The peak position FWHM and %mass concentration of Ni $2p_{3/2}$ .....	53
Table D.1 Conditions used in Shimadzu model GC-14B.....	64

## LIST OF SCHEMES

Scheme 1.1 Diagram of research methodology .....	3
Scheme 4.1 Flow diagram of ethanol dehydrogenation process.....	24



## CHAPTER 1

### INTRODUCTION

Biomass is a renewable and abundant resource especially in Thailand, which is an agricultural country. Rice bran (Figure 1.1), which is one byproduct from the milling process, can apply to make extracted oil in the rice bran oil industry. Finally, it remains rice bran residues which were extracted oil, called deoiled rice bran. Therefore, utilization for adding value to deoiled rice brans which are one of most abundant important renewable material in the country is converting it into activated carbon [1].

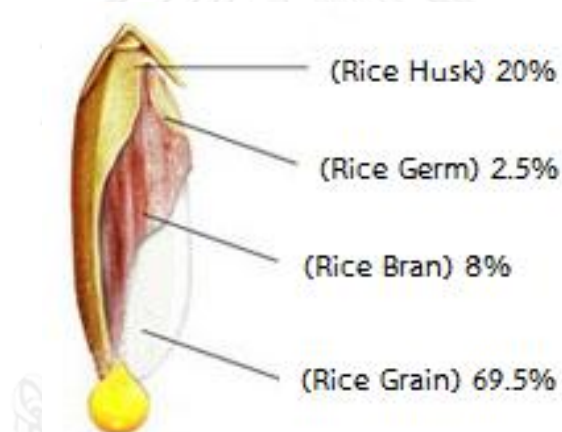


Figure 1.1 Rice seed composition

Activated carbon is broadly used as adsorbent in various industries to treat and purify both gas and liquid because of their suitable porous structure, such as to adsorb heavy metal (such as mercury, chromium and cadmium species) from wastewater or to separate impurity from a contaminated gas [2-4]. Activated carbon is also useful both as catalyst and catalyst support due to its high specific surface area, high thermal and chemical stability and possibility of presence of the basic and acidic character as oxygen functional group on the carbon surface [2, 5, 6].

Dehydrogenation and dehydration of alcohol which are catalyzed by carbon material have not been frequently studied. Even in ethanol, it is converted to acetaldehyde and ethylene associated with dehydrogenation and dehydration

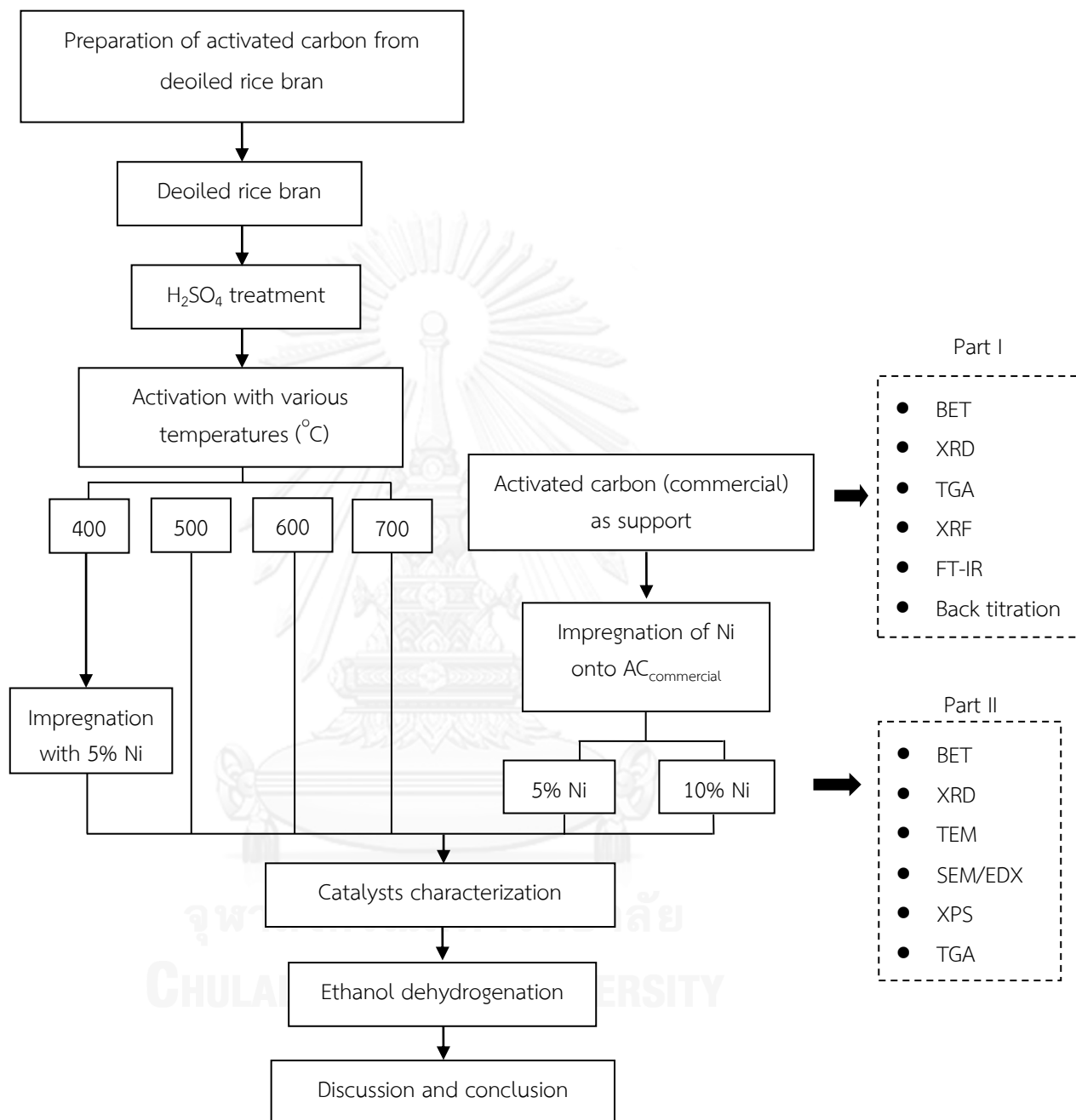
reactions, respectively. Both of the products deserve interest particularly with an acetaldehyde, which is a one of important raw materials in production of chemicals (e.g. acetic acid, acetic anhydride, ethyl acetate, pyridine, vinyl acetate). These chemicals are used for manufacturing plastic, construction materials, fire retardant paints and explosives [7, 8].

To increase the usefulness to deoiled rice bran, it has been prepared into term of carbon material, called activated carbon. Therefore, the objective of this work is to analyze the behavior of activated carbon as catalyst and as catalyst support for nickel catalyst for the dehydrogenation of ethanol to acetaldehyde.

### 1.1 Research scope

1. Synthesize activated carbon from deoiled rice bran
2. Synthesize nickel catalyst supported on activated carbon (commercial grade and prepared from deoiled rice bran) by the impregnation method.
3. Characterize activated carbons with BET, XRD, TGA, XRF, standard back titration and FT-IR
4. Characterize nickel catalysts with BET, XRD, TEM, SEM/EDX, TGA, and XPS
5. Examine the catalytic activity of both activated carbon and nickel supported on activated carbon for the ethanol dehydrogenation.

## 1.2 Research methodology



Scheme 1.1 Diagram of research methodology

## CHAPTER 2

### THEORIES

#### 2.1 Activated carbon

Activated carbon or porous carbon also known as activated charcoal is a form of carbon that has been processed with oxygen to make the tiny pores between the carbons atoms. Therefore, the large surface area of activated carbon, as excess of  $500 \text{ m}^2/\text{g}$ , is the result of the porosity of carbon network. Base on IUPAC, pore diameter can be classified into 3 groups as follows:

- Micropores width less than 2 nm
- Mesopores width between 2 and 50 nm
- Macropores width greater than 50 nm

For micropores, it has also been classified further into ultra (<0.5 nm width) and super-(1.0-2.0 nm) micropores. Generally, microporous is considered to control the size of adsorbent molecule which related to the adsorption behavior. Mesoporous, which is characterized by hysteresis loop during adsorption and desorption of liquid nitrogen ( $-196^\circ\text{C}$ ) at high relative pressure, do not role as large as micropore for adsorption process. Macroporous has not been emphasized for the surface chemist. All activated carbon contains micropore, mesopore and/or macropore within their structure which its proportion of pore structure depend on its nature of raw material.

Due to its high specific surface area, so activated carbons are the suitable material for gas and liquid-phase adsorption process. For example, it is used to remove to heavy metal from wastewater, separate impurities from mixing gas or even to extract gold and silver from low-grade ores in metallurgical industry [2, 9].

### 2.1.1 Production of activated carbon

Activated carbon is usually derived from charcoal. Nevertheless, it can be made from many carbonaceous source materials such as wood, coconut shell, coffee beans, rice husk or even pulp mill residues. General process to produce activated carbon is made through one of following process:

Physical activation: consists basically in a thermal treatment, which occurs in two stages.

*Carbonization:* a carbonaceous source material is pyrolyzed at a high temperature, usually range temperature 600-900°C, in absence of oxygen (usually in inert atmosphere with gas like argon or nitrogen) to create a char.

*Oxidation or Activation:* the char is exposed to oxidizing atmosphere (such as oxygen, steam, carbon dioxide or even their mixture) at temperature above 250°C, usually temperature range 600-1200°C.

Chemical activation: involves addition the certain chemical to raw material to develop the porosity of materials.

Briefly, the carbon source material is impregnated with some chemicals such as an acid, a strong base or a salt. Phosphoric acid, zinc chloride and potassium hydroxide/carbonate are frequently used as chemical agent. Then, the impregnated materials are carbonized at a low temperature, usually temperature range 450-900°C. It is believed that the carbonization / activation step proceeds simultaneously. However, after chemical activation process, activated carbons must be washed to remove the remaining chemical, which may be a cause of poison in some process.

Generally, physical activation process can be produce high yield quality activated carbon compared with chemical activation process. However, physical activation process requires more heat to produce activated carbon that cause of its high cost. Therefore, chemical activation process which required lower temperature is often method for activated carbon production. Moreover, chemical activation process also uses time for production shorter than that one. As sometime, the



combination method (physical activation combine with chemical activation) is employed to develop the porosity of carbon as a desired activated carbon [5, 10].

### 2.1.2 Type and its application of activated carbon

Activated carbon is complex products which are difficult to classify on the basis of their behavior, surface characteristics and preparation methods. Generally, activated carbon can be classified based on their physical characteristic into three main types.

- Powdered activated carbon (PAC) is pulverized carbon with a size less than 0.18mm (US Mesh 80). These are used for purification, deodorizing and de-colouring of foods, chemicals and pharmaceuticals. PAC is also utilized in municipal waste water treatment.
- Granular activated carbon (GAC) is irregular shaped particles, which has larger particle size than PAC, with sizes ranging from 0.2 to 5 mm. The utilization of this activated carbon is in similar application with PAC which is employed in wastewater treatment.
- Extruded activated carbon (EAC) is extruded and cylindrical shaped with diameters from 0.8 to 5 mm. These are mainly used for gas phase applications because of their low pressure drop, high mechanical strength and low dust content.

### 2.1.3 Activated carbon in catalytic process

As sometimes, activated carbon has also been used as a catalyst or a catalyst support for the heterogeneous catalytic process. Resulting from its inertness, activated carbon is widely used as catalyst support because it has been confirmed that the carbon-active site interaction is weak and the behavior of the catalyst is basically controlled by the chemical nature of the active phase. Moreover, its high specific surface area and porous structure are suitably used for well metal dispersion which is very necessary for high catalytic activity.

Actually, activated carbon contains heteroatoms (mainly oxygen, hydrogen and nitrogen) and some inorganic mineral which should have in the nature of carbon. All of these heteroatoms influence the properties of carbon in several ways but the greatest influence come from the presence of oxygen, in particular edge-bonded-oxygen which called oxygen functional group. Oxygen functional group can be founded on carbon surface in several types which is shown in Figure 2.1. The consequence of the presence of oxygen functional group is acidic/basic character of carbon materials which can vary by different pre-treatment condition. Moreover, the origin of these surface groups may depend on the original raw material or even post-treatment after activation process. Therefore, the carbon surface may not as inert as before [2, 9-12].

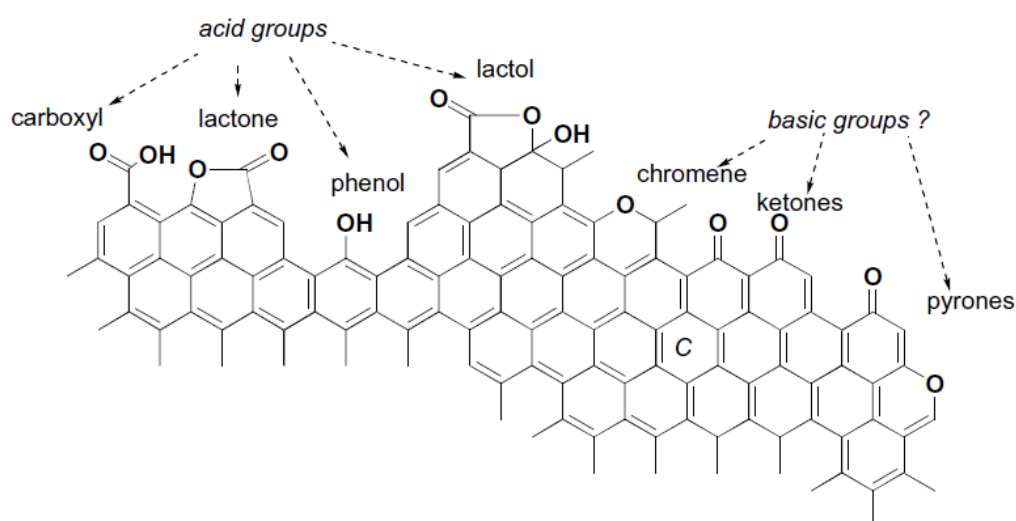


**Figure 2.1 Structure of oxygen functional group on carbon surfaces**

For inorganic impurities (such as calcium, potassium, alumina, silica, sulfur and other heavy metal), it may change the acidic/basic character or redox properties of carbon materials [2, 12]. Although, activated carbon used as catalyst is not so often as catalyst support but there are many reaction which use carbon materials as catalysts, as shown in Table 2.1.

Table 2.1 some reaction catalyzed by carbon

General type	Examples
Reactions involving hydrogen	$RX + H_2 \rightarrow RX$ (X = Cl, Br) $HCOOH \rightarrow CO_2 + H_2$ $CH_3CHOHCH_3 \rightarrow CH_3COCH_3 + H_2$
Reactions involving oxygen	$SO_2 + (1/2)O_2 \rightarrow SO_3$ $NO + (1/2)O_2 \rightarrow NO_2$ $2H_2S + O_2 \rightarrow S_2 + 2H_2O$ Catalytic oxidation of inorganic anions
Reactions involving oxygen	$CO + Cl_2 \rightarrow COCl_2$ $C_2H_4 + 5 Cl_2 \rightarrow C_2Cl_6 + 4HCl$ $SO_2 + Cl_2 \rightarrow SO_2Cl_2$ $C_6H_5CH_3 + Cl_2 \rightarrow C_6H_5CH_2Cl + HCl$

## 2.2 Nickel and Nickel oxide

Nickel (chemical symbol: Ni) has atomic number and atomic weight as 28 and 58.69, respectively. Nickel belongs to transition metal and its crystal structure is face-centered cubic with lattice parameter of 0.352 nm. Nickel is ferromagnetic at ordinary temperature which can preserve in the form of magnetic up to temperature as 350. In general, the ore is transformed to dinickel trisulfide ( $Ni_2S_3$ : oxidation state of nickel is +3), which is roasted in air to give nickel oxide ( $NiO$ : oxidation state of nickel is +2). Finally, nickel oxide is reduced with carbon to form the metal. Physical properties of nickel can be seen in Table 2.2.

Nickel is used either as the pure metal or in the form of alloy such as stainless steels, which are alloy with iron. In addition, resulting from its slowly rate oxidation at room temperature, nickel is used as corrosion-resistant material for coating on other material. Moreover, nickel can also be catalyst for hydrogenation of unsaturated organic compound, such as fats and oils. Although, in its compound has several oxidation state (with -1, 0, +1, +2, +3 and +4) but the most common is  $Ni^{2+}$ . There are many nickel compounds which is nickel state as +2 such as  $NiCl_2$ ,  $Ni(NO_3)_2 \cdot 6(H_2O)$ ,  $NiO$  or even  $Ni_2O_3$ . Natural nickel consists of five stable isotopes: nickel-58

(68.27 percent), nickel-60 (26.10 percent), nickel-61 (1.13 percent), nickel-62 (3.59 percent) and nickel-64 (0.91 percent).

**Table 2.2 Physical properties of nickel**

properties	value
Atomic number	28
Atomic weight (amu)	58.69
Electron configuration	[Ar] 4s <sup>2</sup> 3d <sup>8</sup> or [Ar] 4s <sup>1</sup> 3d <sup>9</sup>
Density (g/cm <sup>3</sup> )	8.908
Liquid density at melting point (g/cm <sup>3</sup> )	7.81
Melting point (°C)	1455
Boiling point (°C)	2913
Heat of fusion (kJ/mol)	17.48
Heat of vaporization (kJ/mol)	377.5
Molar heat capacity (J/mol · K)	26.07
Electrical resistivity at 20°C (nΩ · m)	69.3
Thermal conductivity (W/m · K)	90.9
Thermal expansion at 25°C (μm/ m · K)	13.4
Young's modulus (GPa)	200
Shear modulus (GPa)	76
Bulk modulus (GPa)	180

Actually, nickel has two oxides: Nickel (II) oxide (with the formula NiO) and Nickel (III) oxide (with Ni<sub>2</sub>O<sub>3</sub> or NiO<sub>2</sub>) but NiO is widely acknowledged as oxide of nickel, which is classified as a basic metal oxide. Nickel (II) oxide, NiO is formed when nickel powder reacts with oxygen at above temperature 400°C. Conversely, NiO is reduced to form metallic nickel in the presence of hydrogen, carbon or carbon monoxide.

## 2.3 Decomposition of alcohol

Decomposition of alcohols which consists of dehydrogenation and dehydration is used to investigate the character of catalysts. As follow from previous literatures, many researchers had such attempt to justify the behavior of these reactions with different catalysts. Mostly, it is presumed that dehydration of alcohol associated with acid site while dehydrogenation prefer to presence of basic character of catalysts. Nevertheless, dehydrogenation also takes place on metal oxide as redox centre.

### 2.3.1 Dehydrogenation of alcohols

Dehydrogenation of alcohols means the removal of two hydrogen atoms from an alcohol molecule. In formal, a primary alcohol is dehydrogenated to an aldehyde whereas a secondary alcohol is dehydrogenated to a ketone.

Actually, the conversion of alcohols into carbonyl compounds can be achieved by catalytic dehydrogenation or by chemical oxidation. Catalytic dehydrogenation is especially of advantage with primary alcohols because it prevents over oxidation to carboxylic acids. Moreover, the vapor-phase dehydrogenations are applicable only to the preparation of aldehydes that tolerate such high temperature [13, 14].

The dehydrogenation of ethanol, which is primary alcohol, to acetaldehyde and hydrogen is an endothermic reaction as shown in equation[15]:



### 2.3.2 Dehydration of alcohols

Dehydration of alcohols is an elimination of water from an alcohol which is illustrated by Figure 2.2 as example.

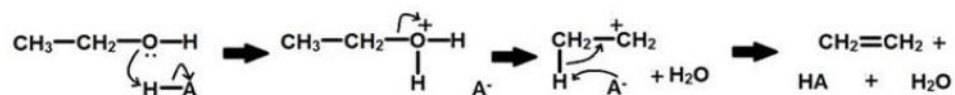


Figure 2.2 Mechanism for the dehydration of ethanol to ethylene

The mechanism of ethanol dehydration to ethylene was shown in Figure 2.2. Acid catalysts first protonates the hydroxyl group on ethanol, which leaves as a water molecule. Then, conjugate base of the catalyst deprotonates the methyl group and the hydrocarbon rearranges into ethylene. The dehydration of ethanol to generate ethylene is an endothermic reaction. Hence, at high temperature ethylene is generated as main product. Conversely, ether which is main byproduct, are often generated at low temperature [16, 17].

CHAPTER 3  
LITERATURE REVIEWS

3.1 Activated carbon

As well know that the properties of activated carbon (such as porosity and specific surface area) depend on various factors such as the nature of raw material, activation process or even condition used for preparation of activated carbon [2]. The properties of activated carbon obtained from different raw material or activation process is summarized in Table3.1 as example.

**Table 3.1 Main characteristic of different activated carbon at optimum condition**

precursor	Activation process	The properties of activated carbon		
		$S_{BET}$ ( $m^2/g$ )	$V_{mic}$ ( $cm^3/g$ )	Yield (%)
Cherry stones[18]	ZnCl <sub>2</sub> activation			
	-carbonization temperature 400°C	1472	0.67	-
	-carbonization temperature 800°C	992	0.49	-
Pomegranate seed[19]	ZnCl <sub>2</sub> activation	978	0.28	39.2
Olive stone[6]	Steam activation	914	0.51	-
Coconut shell char[20]	Steam activation	-	0.50	-
Olive stone[7]	H <sub>3</sub> PO <sub>4</sub> activation			
	-carbonization temperature 400°C	1628	0.68	41.9
	-carbonization temperature 800°C	1294	0.57	35.9

There are many researches to show that activated carbons are suitably used as adsorbent and catalysts support [2]. For example, Auer E. et al. [12] reported that activated carbon supported palladium catalyst was widely used in liquid phase aromatic ring hydrogenation, dehydrogenation or oxidation of alcohols, reductive

amination or even debenzylolation reaction. Meanwhile, Sato S. et al. [21] showed that carbon material which made from coal can remove the cadmium(II) and zinc(II) ions as heavy metal from aqueous solution.

### 3.2 Dehydrogenation of alcohol over metal catalysts

Dehydrogenation of alcohol to carbonyl compound (primary alcohols are oxidized to aldehydes whereas secondary alcohols are oxidized to ketones) have been frequently studied over several transition metal catalysts. Because it is well known that transition metal oxide can act as catalyst for dehydrogenation reaction [22].

In 2003, Chang F.-W. et al. [15] studied the catalytic behavior of copper catalysts on rice husk ash prepared by incipient wetness impregnation ( $\text{Cu/RHA}_m$ ) on the dehydrogenation of ethanol. They found that the initial conversion increased from about 70 to 78% with increasing percentage metal loading from 1 to 10 wt% at reaction temperature 523 K and selectivity of acetaldehyde was assumed to be 100%. Hence, they concluded that the rate of ethanol dehydrogenation may depend on the surface area of copper metal. Moreover, they studied effect of the reaction temperature over 5wt% $\text{Cu/RHA}_m$  and found that ethanol conversion increased from 68% to 81% with increasing the reaction temperature from 473 to 573 K. However,  $\text{Cu/RHA}_m$  was rapidly deactivated. The cause of deactivation of the  $\text{Cu/RHA}_m$  catalyst may result from sintering of copper metal. Therefore, in a few years later, they prepared copper catalysts on rice husk ash by ion exchange method ( $\text{Cu/RHA}_x$ ) to compare the effect of preparation method of  $\text{Cu/RHA}$ . This study found that the initial conversion over  $\text{Cu/RHA}_x$  catalyst, increased with increasing Cu loading. This result was similar trend with their recent work. In addition, ethanol conversion over 5.75wt% $\text{Cu/RHA}_x$ , increased from 22.1 to 77.0% with increasing the reaction temperature from 483 to 548 K. The deactivation of this catalyst was very low. In summary, they reported that  $\text{Cu/RHA}$  catalyst prepared by ion exchange is more stable than  $\text{Cu/RHA}$  catalyst prepared by incipient wetness impregnation. Moreover,



they proposed that surface  $\text{Cu}^{(0)}$  species were responsible for ethanol dehydrogenation [23].

El-Molla S.A. et al. [22] studied catalytic conversion of isopropanol to acetone or propene (as dehydrogenation and dehydration, respectively) over various transition metal oxides (cobalt, copper and nickel oxide) supported on activated carbon. They found that all catalyst exhibited very activity for dehydrogenation of isopropanol (at reaction temperature range 150 to 250°C), with selectivity of acetone of above 90%. For dehydration of isopropanol, selectivity of propene was less than 5%. The treating activated carbon with 5% transition metal oxide increased the total conversion as compared to original activated carbon. However, if catalysts were treated with high loading metal up to 10%, the total conversion was decreased. CuO catalysts (both of 5%CuO/AC and 10%CuO/AC) showed the highest total conversion of isopropanol as compared to other metal oxide catalysts. At highest reaction temperature (250°C), the total conversion was about 75% when used CuO/AC as catalysts.

Neramittagapong A. et al. [8] reported nickel catalyst supported on  $\text{SnO}_2$ ,  $\text{Al}_2\text{O}_3$  and  $\text{SiO}_2$  for acetaldehyde production from ethanol. They found that Ni/ $\text{SnO}_2$  catalyst showed the highest conversion and selectivity of acetaldehyde as compared to other nickel catalyst which supported on  $\text{Al}_2\text{O}_3$  and  $\text{SiO}_2$  (under condition: reaction temperature 200-350°C, 5 wt% Ni loading). For 5%Ni/ $\text{SiO}_2$ , the maximum ethanol conversion was 41.48%, with acetaldehyde selectivity of 83.73% when reaction temperature was 300°C. In addition, they also found that the conversion obviously increased with increasing metal loading up to 10%wt. Even if catalysts were loaded Ni as excess of 10%, the conversion was constant. Meanwhile, Badlani M. and I.E. Wachs [24] reported that NiO could promote the dehydrogenation of methanol to formaldehyde.

### 3.3 Dehydrogenation of alcohol over surface-treated activated carbon

According to previous chapter, activated carbon can act as acidic and/or basic catalysts which are associated with oxygen functional group on carbon surface. However, the oxygen functional group can be introduced by surface treatment or also called oxidizing treatment. Therefore, many research workers studied the acid/basic character of activated carbon through dehydrogenation and dehydration of alcohols.

Carrasco-Marin F. et al. [6] studied activity of carbon catalysts prepared by oxidizing treatment with  $(\text{NH}_4)_2\text{S}_2\text{O}_8$  by different period of time for dehydrogenation and dehydration of ethanol. They found that ethanol conversion increased with the oxidation time. Oxidized carbons were able to give both dehydrogenation and dehydration reaction. Ether was main product, with selectivity of about 60%. They also reported that ether was unstable under reaction condition (453 K, He/ethanol) hence it was decomposed to ethene as show below

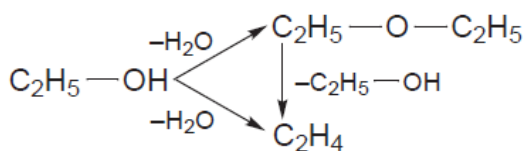


Figure 3.1 Proposed the formation partway of ether and ethene form ethanol dehydration on oxidized carbon

Both dehydrogenation and dehydration rate (measured by activity for acetaldehyde and ethene /ether formation, respectively) increased with rise in the total surface acidity, which was consequence of an increase in oxidizing time. However, dehydrogenation also takes place on original activated carbons, which were basic catalyst. Therefore, they concluded that dehydration reaction only take place on acid surface sites of the Brönsted type. Dehydrogenation can occur both basic and acid surface group.

In a few years later, Moreno-Castilla C. et al. [25] studied activated carbons oxidized with different agent ( $\text{H}_2\text{O}_2$ ,  $(\text{NH}_4)_2\text{S}_2\text{O}_8$ ,  $\text{HNO}_3$ ) for dehydration of methanol to dimethyl ether. They found that carbon catalysts which oxidized with  $(\text{NH}_4)_2\text{S}_2\text{O}_8$  showed highest activity because it had strongest acid group.

Jasinska E. et al. [26] studied decomposition (dehydration and dehydrogenation) of isopropanol over activated carbon modified with different chemical agents ( $\text{HNO}_3$ ,  $\text{H}_2\text{SO}_4$ , peroxyacetic acid (PAA), air,  $\text{NH}_3$  and  $\text{Cl}_2$ ). They found that the method of modification of the activated carbon affects to the conversion and selectivity of this reaction. Isopropanol were dehydrogenated to acetone and dehydrated to propylene. Carbon catalysts which was modified with  $\text{HNO}_3$  for 8 h ( $\text{K}/\text{HNO}_3/8$  h) showed highest activity for dehydration of isopropanol because these catalysts had the largest amount of oxygen(which indicated as carboxyl group) as compared to others catalysts. Conversion of isopropanol for dehydration was over 90%. This result agreed with report of Szymanski G.S. et al. [27], which proved that dehydration needs carboxyl group of different strength. Dehydrogenation reaction occurs simultaneously on Lewis basic and acidic centers.

In addition, it is seen that activated carbon modified with  $\text{Cl}_2$  and  $\text{NH}_3$  can promote dehydrogenation more than dehydration of isopropanol. In contrast, carbon modified with  $\text{H}_2\text{SO}_4$  and air can act as catalysts in dehydration than dehydrogenation reaction [26].

At previous literature review, the dehydrogenations of alcohols frequently take place along with dehydration reaction over carbon catalysts. Therefore, studying the dehydration of alcohols is important for studying the dehydrogenations of alcohols.

Bedia J. et al. [28] studied catalytic behavior of carbon catalysts treated with different chemical agent on isopropanol decomposition. PAC and SAC (activated carbon treated with  $\text{H}_3\text{PO}_4$ ,  $\text{H}_2\text{SO}_4$ , respectively) which were the acidic carbons, only take place dehydration toward propylene, with propylene selectivity of 100% at isopropanol conversion of 60%. BaAC and CaAC were activated carbon treated with  $\text{Ca}(\text{OH})_2$ ,  $\text{Ba}(\text{OH})_2$ , respectively. BaAC catalyst showed high selectivity of acetone of

about 80%, which were product from dehydrogenation reaction. For CaAC catalysts, selectivity of propylene was 73% and acetone was 27%. Summarizing, CaAC contained both basic and acidic site.

Activated carbon which prepared by chemical activation with  $\text{H}_3\text{PO}_4$  have been studied as catalyst for dehydration of 2-propanol to propylene [5]. Bedia J. et al. reported that amount of phosphorus which remains in catalyst surface after the washing process, promoted catalytic performance in term of conversion. They presumed that phosphorus may act as a Brønsted acid. Afterwards, they also studied catalytic activity of activated carbon which prepared by chemical activation with  $\text{H}_3\text{PO}_4$  on ethanol dehydration [7]. They found that high activation temperature and high impregnation ratio ( $\text{H}_3\text{PO}_4$  /precursor) were cause of amount of phosphorus enhancement. Therefore, HA2-800, which has highest phosphorus concentration, showed highest conversion. The main product from ethanol dehydration at high reaction temperature was ethylene.

### 3.4 Nickel catalyst supported on activated carbon

Nickel supported on activated carbon has been used in several reactions. Bradford M.C. and M.A. Vannice [29] reported that type of support had influence to catalytic reforming of methane with carbon dioxide over nickel catalyst. They found that specific activity on a turnover frequency (TOF) basis obtained from all catalysts was sequence as follow:  $\text{Ni}/\text{TiO}_2 > \text{Ni}/\text{C} > \text{Ni}/\text{SiO}_2 > \text{Ni}/\text{MgO}$ . Wang S. and G. Lu [30] studied  $\text{Ni}/\text{AC}$  which activated carbon treated with difference acid ( $\text{HCl}$ ,  $\text{HNO}_3$ ,  $\text{HF}$ ) and found that the crystallite size of Ni depend on acid treatment which sequenced as follow  $\text{Ni}/\text{AC}-\text{HCl} > \text{Ni}/\text{AC}-\text{HF} > \text{Ni}/\text{AC}-\text{HNO}_3$ . However, all acid-treated carbons showed low conversion and specific activities in  $\text{CO}_2/\text{CH}_4$  reforming reaction.

Zielinski M. et al. [31] showed performance of  $\text{Ni}/\text{AC}$  catalysts for hydrogen storage. They found that type of nickel precursor had influence metal surface area. The metal surface area from  $\text{Ni}/\text{AC}-\text{A}$  ( $\text{Ni}(\text{CH}_3\text{COO})_2 \cdot 4\text{H}_2\text{O}$  as precursor) and  $\text{Ni}/\text{AC}-\text{N}$  ( $\text{Ni}(\text{NO}_3)_2 \cdot 6\text{H}_2\text{O}$  as precursor) was about 2 and 15  $\text{m}^2/\text{g}_{\text{Ni}}$ , respectively. Moreover,

Ni/AC showed high performance for hydrogen storage, with H<sub>2</sub> up to 53 wt% (at room temperature and 30 bars).



## CHAPTER 4

### EXPERIMENTAL

#### 4.1 Preparation of activated carbon derived deoiled rice bran

To study the effect of activation temperature on carbon material used as catalyst in ethanol dehydrogenation, so the carbon catalysts will be prepared in various activation temperatures, which are 400, 500 600 and 700°C.

##### 4.1.1 Chemical

1. Sulphuric acid ( $\text{H}_2\text{SO}_4$ )
2. Sodium bicarbonate ( $\text{NaHCO}_3$ )
3. Zinc chloride ( $\text{ZnCl}_2$ )
4. Hydrochloric acid (HCl)
5. Distilled water

##### 4.1.2 Experimental procedure

Deoiled rice brans as obtained from Thai Edible Co.Ltd., were used as the raw material in the preparation of activated carbon.

1. Deoiled rice bran was treated with concentrated sulphuric acid (at deoiled rice bran to  $\text{H}_2\text{SO}_4$  weight ratio of 1:1) at 150°C for 24 h. Then, the material was cooled followed by ground.
2. To eliminate the excess acid on carbon material, the sample was washed with sodium bicarbonate solution (1% weight/volume) until neutral. Then, the sample was washed with distilled water and dried at 110°C for 24 h.
3. The resulting sample was impregnated with zinc chloride (at the resulting carbon material to  $\text{ZnCl}_2$  weight ratio of 1:1) and dried at 110°C for 24 h.

4. The impregnated sample was activated under nitrogen atmosphere with flow  $N_2$  flow rate of 200 ml/min and ramp rate of  $10^\circ\text{C}/\text{min}$ . When reached desired temperature (400, 500, 600 and  $700^\circ\text{C}$ ), the sample was held at this temperature for 1 h. After that these samples were cooled down to room temperature.
5. The samples were stirred with hydrochloric acid solution (1M HCl) at  $70^\circ\text{C}$  for 6 h. followed by washing with distilled water several times to remove the remaining chemical on these samples.
6. Finally, the samples were dried at  $110^\circ\text{C}$  for 24 h.

#### 4.1.3 The nomenclature of samples

The carbon catalysts were denoted as AC\_X

Where AC is activated carbon derived from deoiled rice bran and

X is activation temperature,  $^\circ\text{C}$ .

For example, AC\_400 is activated carbon derived from deoiled rice bran activated with temperature  $400^\circ\text{C}$ .

## 4.2 Preparation of activated carbon supported nickel catalyst

Nickel catalysts supported on activated carbon were prepared by incipient impregnation method.  $\text{Ni}(\text{NO}_3)_2 \cdot 6\text{H}_2\text{O}$  was used as nickel precursor. In this study, the percentage of nickel loading was 5 and 10.

### 4.2.1 Chemical

1. Activated carbon used as support
  - commercial grade: SIGMA-ALDRICH DARCO<sup>®</sup>, 12-20 mech. Granular
  - activated carbon derived from deoiled rice bran

2. Nickel(II) nitrate hexahydrate ( formula:  $\text{Ni}(\text{NO}_3)_2 \cdot 6\text{H}_2\text{O}$  ) as nickel precursor
3. De-ionized water

#### 4.2.2 Experimental procedure

1.  $\text{Ni}(\text{NO}_3)_2 \cdot 6\text{H}_2\text{O}$  which has amount of nickel percentage as desired, was dissolved in de-ionized water. The volume of this solution has to equal in the pore volume of activated carbon.
2.  $\text{Ni}(\text{NO}_3)_2 \cdot 6\text{H}_2\text{O}$  solution was slowly dropped into activated carbon
3. The impregnated materials were dried at  $110^\circ\text{C}$  for 24 h.
4. Finally, the samples were calcined in air at  $400^\circ\text{C}$  for 2 h.

#### 4.2.3 The nomenclature of samples

The nickel catalysts supported on activated carbon were denoted as Y%Ni/Z,

Where Y is the percentage of nickel loading, % and

Z is activated carbon used as support (commercial grade or derive from deoiled rice bran)

For example, 5%Ni/AC<sub>C</sub> is 5% nickel supported on activated carbon grade commercial or 5%Ni/AC<sub>400</sub> is 5% nickel supported on activated carbon derive from deoiled rice bran activated with temperature  $400^\circ\text{C}$ .

### 4.3 Characterization of catalysts

The catalyst was characterized by a variety of techniques as shown below.

#### 4.3.1 Nitrogen adsorption-desorption isotherm

The catalysts approximately 50 mg was measured specific surface area, pore volume and pore diameter by  $\text{N}_2$  adsorption-desorption at liquid nitrogen ( $-196^\circ\text{C}$ ) using a Micromeritics ASAP 2000 instrument. The surface area and pore size



distribution was calculated by Brunauer-Emmelt-Teller (BET) and BJH method, respectively.

#### **4.3.2 X-ray diffraction (XRD)**

X-ray diffraction (XRD) was used to observe the carbon structure of activated carbon and the dispersion of nickel species on carbon material by a SIEMENS D5000 X-ray diffractometer using  $\text{CuK}\alpha$  radiation with Ni filter in the  $2\theta$  range of 10-80 degrees resolution  $0.04^\circ$ .

#### **4.3.3 Thermal Gravimetric analysis (TGA)**

Thermal Gravimetric analysis (TGA) was used to study the thermal decomposition of catalyst under the temperature range of room temperature to  $1000^\circ\text{C}$  with a heating rate of  $10^\circ\text{C}/\text{min}$  in nitrogen atmosphere using an STD analyzer model Q600 from TA instrument.

Moreover, TG/DTA analysis also used to investigate the decomposition of nickel catalysts during the calcination, the thermal decomposition of the catalysts precursor is also studied by in situ TGA/DTA analysis under the room temperature to  $600^\circ\text{C}$  in air with a heating rate of  $10^\circ\text{C}/\text{min}$ .

#### **4.3.4 X-ray fluorescence spectrometer (XRF)**

X-ray fluorescence spectrometer was performed to determine a variety of impurities in activated carbon. Model of XRF: Phillips model PW2400 at the Scientific and Technological Research Equipment Center, Chulalongkorn University (STREC). Amount of impurities were estimated by using theoretical formular, "Fundamental parameter calculation".

#### **4.3.5 Fourier transforms infrared spectroscopy (FT-IR)**

FT-IR analysis was used to determine the functional group as the chemical structure of activated carbon using a Nicolet 6700 FTIR spectrometer.

#### 4.3.6 Scanning Electron Microscopy (SEM) and Energy dispersive X-ray spectroscopy (EDX)

Scanning electron microscopy (SEM) and Energy dispersive X-ray spectroscopy (EDX) were used to determine the morphology and elemental distribution of catalysts. Model of SEM: JEOL mode JSM-5800LV and EDX was performed using Link Isis Series 300 program at the Scientific and Technological Research Equipment Center, Chulalongkorn University (STREC).

#### 4.3.7 X-ray photoelectron spectroscopy (XPS)

XPS analysis was used to calculate the chemical composition at around surface of catalysts. This technique was performed by an AMICUS spectrometer using MgK $\alpha$  X-ray radiation at voltage 15kV and current of 12 mA. The pressure in the analysis chamber was less than  $10^{-5}$  Pa.

#### 4.3.8 Standard back titration

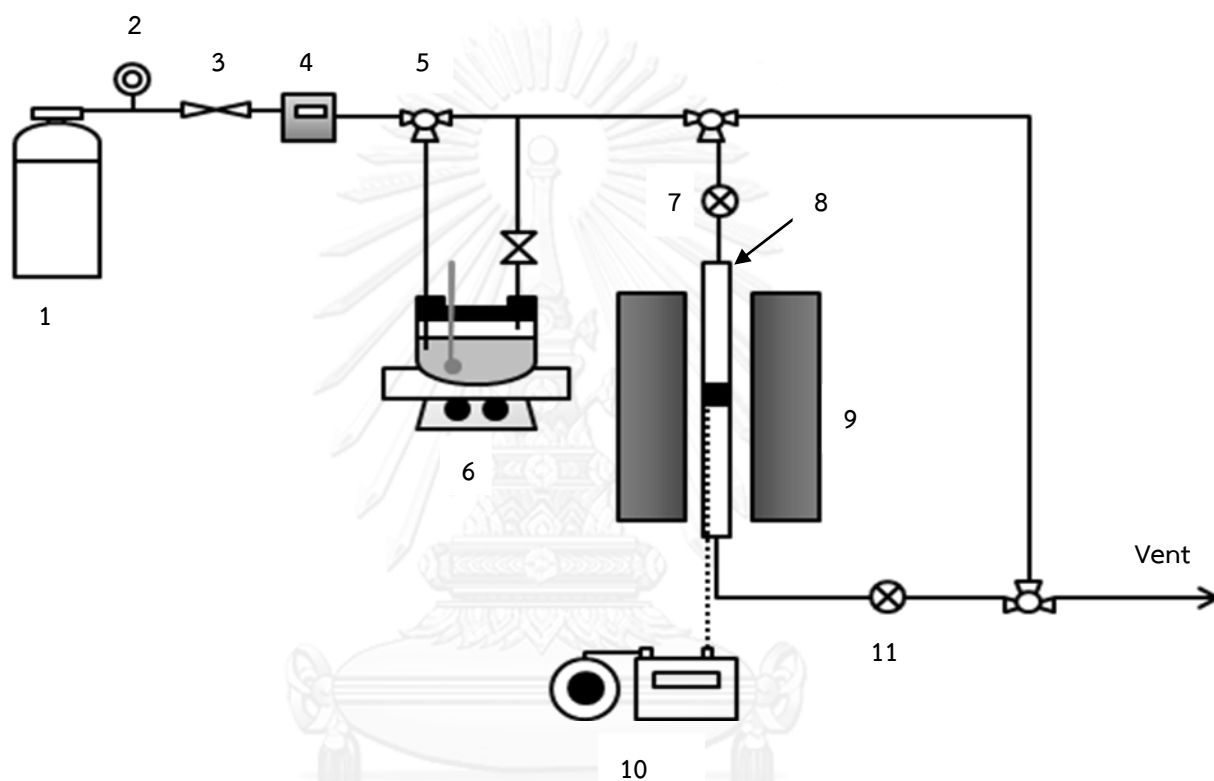
The total acid density of the catalysts was obtained using standard acid-base back titration. Typically, approximately 0.1 g of carbon catalyst was stirred with NaOH solution (30 ml, 0.004 M) at room temperature for overnight. Then, the excess NaOH was neutralized with HCl solution (0.02 M).

#### 4.3.9 Transmission Electron Microscopy (TEM)

TEM analysis was used to observe the morphology and the crystallite size of nickel by using JEOL JEM 2010 operating at 200 kV.

#### 4.4 Measurement of catalytic activity with ethanol dehydrogenation

Catalytic behavior of catalysts on the dehydrogenation of ethanol will be performed in vapor phase at atmospheric pressure in a micro-tubular fixed bed reactor made from glass with 7 mm inside diameter. The ethanol dehydrogenation diagram is shown in Scheme 4.1.



- |                       |                      |                            |
|-----------------------|----------------------|----------------------------|
| 1. Argon gas          | 5. 3-way valve       | 9. Electrical furnace      |
| 2. Pressure regulator | 6. Ethanol saturator | 10. Temperature controller |
| 3. On-off valve       | 7. Sampling point    | 11. Heating coil region    |
| 4. Argon flow meter   | 8. Tubular reactor   |                            |

**Scheme 4.1** Flow diagram of ethanol dehydrogenation process

Approximately 50 mg of catalyst was packed in tubular reactor, which has quartz wool as bed with 0.5 cm bed length in the middle of the reactor. The reactor will be placed in electrical furnace. Temperature in furnace was controlled with

automatic temperature controller, which is connected to a thermocouple attached to the catalyst bed in reactor. The procedure of reaction as shown below:

- Pre-heat catalyst

Before run reaction, the catalyst was heated at temperature of 200°C in inert atmosphere using argon flow of 50 ml/min and hold at this temperature for 1 h.

- Ethanol saturation

Ethanol (100 ml) was saturated at temperature of liquid ethanol of 45°C in water bath, which heated up to 63°C. To increase efficiency of ethanol vapor, a few ethanol (30 ml) was also saturated in same condition as second stage. Saturation of ethanol was held for 1 h.

- Reaction

Ethanol in form of vapor was introduced into reactor by flowing argon gas with flow rate 50 ml/min. When the temperature reached to desired temperature, which is ranged from 200-400°C, the exit gas will be taken for analysis by gas chromatograph. To avoid the condensation of all product or reactant, outlet line region was heated by heating coil as controlled at 120°C.

The activity of catalyst for the dehydrogenation of ethanol was considered in terms of ethanol conversion and selectivity of main products. The main products are acetaldehyde, ethylene and di-ethyl ether.

- Analysis by gas chromatograph

The concentration of gas products was analyzed by Shimadzu gas chromatograph with flame ionization detector (FID). The condition of FID gas chromatograph was shown in Table 4.1

Table 4.1 Operating condition of gas chromatograph

Gas chromatograph	SHIDAMADZU GC-14B
Detector	FID
Column	
▪ Length (m)	30
▪ Diameter (mm)	0.250
▪ Maximum temperature (°C)	350
Carrier gas	N <sub>2</sub>
Column temperature	
▪ Initial temperature (°C)	40
▪ Final temperature (°C)	40
Detector temperature (°C)	150
Injector temperature (°C)	150

## CHAPTER 5

### RESULTS AND DISCUSSION

This chapter is divided into two parts. The first part explains the characteristics and catalytic activity of activated carbon derived deoiled rice bran for ethanol dehydrogenation. The second part describes characteristics and catalytic activity of nickel catalysts supported on activated carbon.

#### 5.1 Characteristics and catalytic activity of activated carbon derived deoiled rice bran for ethanol dehydrogenation

##### 5.1.1 Nitrogen physisorption

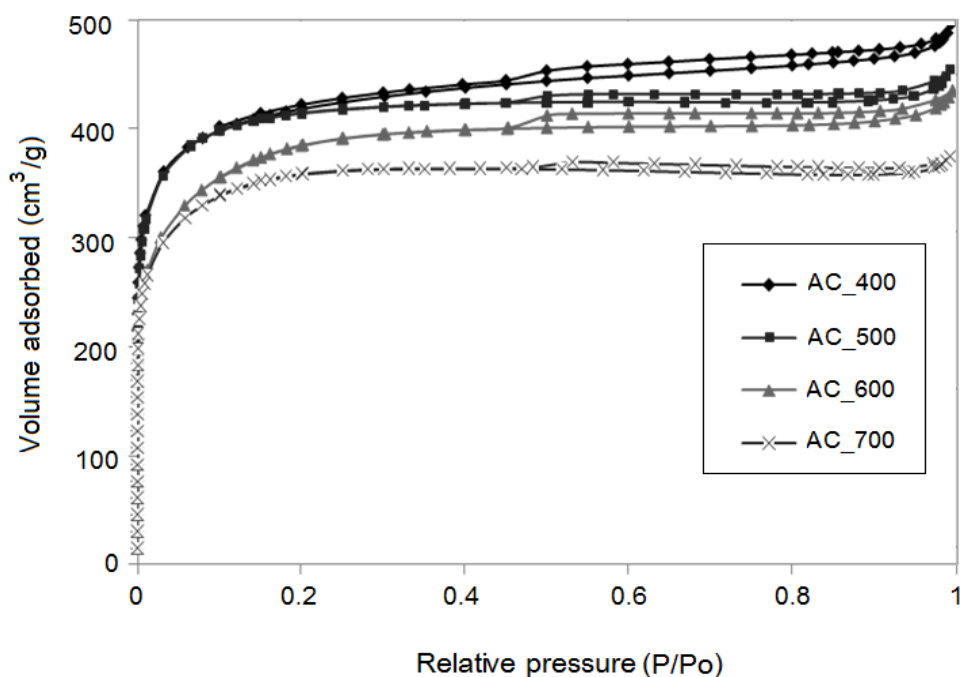


Figure 5.1 N<sub>2</sub> adsorption-desorption isotherms at -196°C of the activated carbon derived deoiled rice bran

The most common procedure for determining the structure of porosity and specific surface area of catalysts is the adsorption-desorption of liquid nitrogen at  $-196^{\circ}\text{C}$ . Figure 5.1 shows the  $\text{N}_2$  adsorption-desorption isotherm of the activated carbons derived deoiled rice bran prepared by various activation temperatures. All catalysts exhibit a *type-I* isotherms (classified by IUPAC: International Union of Pure and Applied Chemistry) which are observed from its adsorption of  $\text{N}_2$  at low relative pressure ( $P/P_0$  values from zero to about 0.05). These isotherms indicate that all catalysts present microporous structure. In addition, all catalysts also display similar isotherm with hysteresis loop (between the adsorption and desorption isotherm) at high relative pressure ( $P/P_0 > 0.4$ ), indicating the formation of mesoporous structure. Consequently, all catalysts are composed of both microporous and mesoporous structure. It is observed that the amounts of  $\text{N}_2$  adsorbed decrease with rising the activation temperature. Activated carbon activated at  $400^{\circ}\text{C}$  (AC\_400 sample) shows the highest nitrogen adsorption capacity which relates to high pore volume.

**Table 5.1 Porous properties of activated carbon from deoiled rice bran**

Catalysts	$S_{\text{BET}}$ ( $\text{m}^2/\text{g}$ )	$V_{\text{total}}$ ( $\text{cm}^3/\text{g}$ )	$V_{\text{mic}}$ ( $\text{cm}^3/\text{g}$ )	$\%V_{\text{mic}}$	$D_p$ (nm)
AC_400	1404	0.746	0.633	84.85	2.126
AC_500	1385	0.686	0.653	95.19	1.981
AC_600	1288	0.659	0.609	92.41	2.049
AC_700	1196	0.569	0.568	99.82	1.905

$S_{\text{BET}}$  = BET surface area;  $V_{\text{mic}}$  = Micropore volume;  $V_{\text{total}}$  = Total pore volume;

$\%V_{\text{mic}} = V_{\text{mic}}/V_{\text{total}} * 100$ ;  $D_p$  = Average pore diameter

The structural parameters obtained from the  $\text{N}_2$  adsorption-desorption are summarized in Table 5.1. These results show that the specific surface area and pore volume of activated carbons decreased with increasing activation temperature from  $400$  to  $700^{\circ}\text{C}$ . The AC\_400 sample exhibits the highest specific surface area and total pore volume which are  $1404 \text{ m}^2/\text{g}$  and  $0.746 \text{ cm}^3/\text{g}$ , respectively. This result show the similar trend with Yorgun S. et al., who studied the activation carbon obtained

from Paylownia wood by using  $\text{ZnCl}_2$ . They reported that the specific surface area and pore volume decreased because of heat shrinking [32]. Moreover, the percentage of microporosity increases from 84.85 to 99.82 with increasing activation temperature. In addition, the pore diameter decreased slightly with increasing activation temperature. The maximum pore diameter is 2.126 nm when activation temperature is  $400^\circ\text{C}$ .

### 5.1.2 X-ray diffraction (XRD)

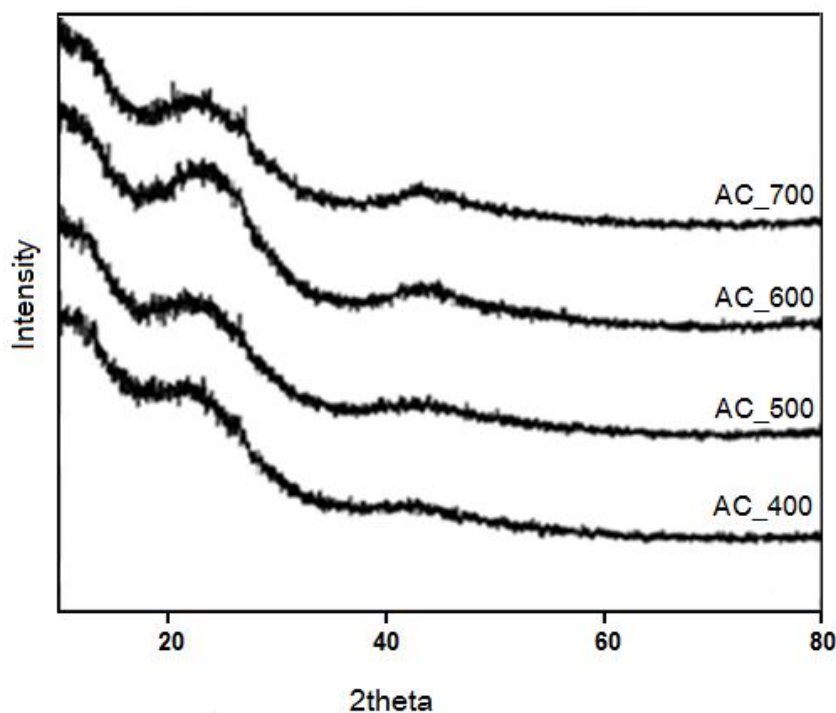


Figure 5.2 XRD patterns of activated carbon catalysts

Figure 5.2 shows XRD patterns of activated carbon catalyst prepared by various activation temperatures. In all sample, there are broad diffraction peak around  $2\theta=22.5$ , which can be denoted as amorphous carbon composed of aromatic carbon sheets [10]. In addition, broad diffraction peak around  $2\theta=45$  which can be defined as graphite structure was raised narrowly with increasing activation temperature. These results indicate that activated carbon catalyst activated at higher



temperature consists of larger carbon sheet than activated carbon catalyst activated at lower temperature.

### 5.1.3 Thermogravimetric and differential thermal analysis (TG/DTA)

The thermal decomposition of activated carbons is observed by using TG/DTA technique under nitrogen atmosphere in which is shown in Figure 5.3. In all catalysts, the weight loss of samples has three stages. In the first stage, the weight loss occurs at temperature below 200°C which could be attributed to water elimination. At the temperature range about 200 to 400°C as second stage, the weight loss is about 5%. It may be attributed to pyrolysis or volatilization of organic molecule. In the third stage, the weight loss occurs at temperature above 400°C, which may be attributed to thermal decomposition and reaction between activating agent and carbonaceous residue [1, 33, 34].

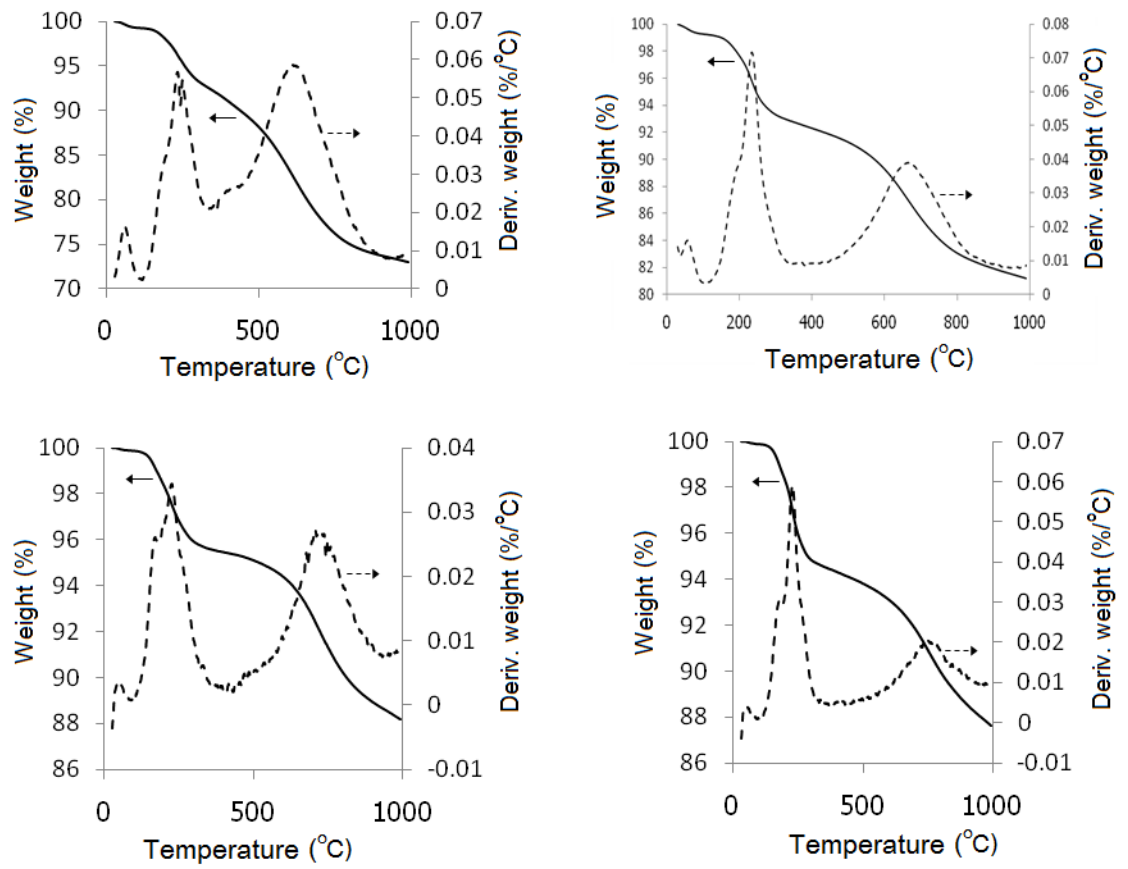


Figure 5.3 Thermal analysis of activated carbon derived deoiled rice bran by various activation temperatures (a) AC\_400 (b) AC\_500 (c) AC\_600 (d) AC\_700

#### 5.1.4 X-ray fluorescence spectrometer (XRF)

Due to activated carbon was prepared by chemical activation hence it may have remaining chemical (even though it was removed during washing step) as impurities. Amount of impurity of carbon materials as shown in Table 5.2 was obtained from XRF analysis.

All catalysts have little amounts of zinc, which increases slightly from 1400 to 1700 ppm with rising activation temperature. In addition, the amount of sulfur also increases clearly from 10300 to 46200 ppm with increasing the activation temperature from 400 to 700°C.

**Table 5.2 Total acid density and amount of impurities of activated carbon**

catalysts	Total acid density <sup>a</sup> ( $\mu\text{mol}/\text{m}^2$ )	amount of impurities <sup>b</sup>	
		Zn (ppm)	S (ppm)
AC_400	0.720	1400	10300
AC_500	0.693	1600	33900
AC_600	0.642	1700	34700
AC_700	0.709	1700	46200

<sup>a</sup> acid-base back titration; <sup>b</sup> examined by XRF

#### 5.1.5 Total acid density

Standard acid-base back titration can be used to examine the total acid density of the catalysts as also shown in Table 5.2. Total acid density of activated carbon catalysts which in order from the greatest to the least as following: AC\_400 > AC\_700 > AC\_500 > AC\_600. It notices that AC\_400 sample is highest total acid density which is 0.720  $\mu\text{mol}/\text{m}^2$ .

### 5.1.6 Fourier transforms infrared spectroscopy (FT-IR)

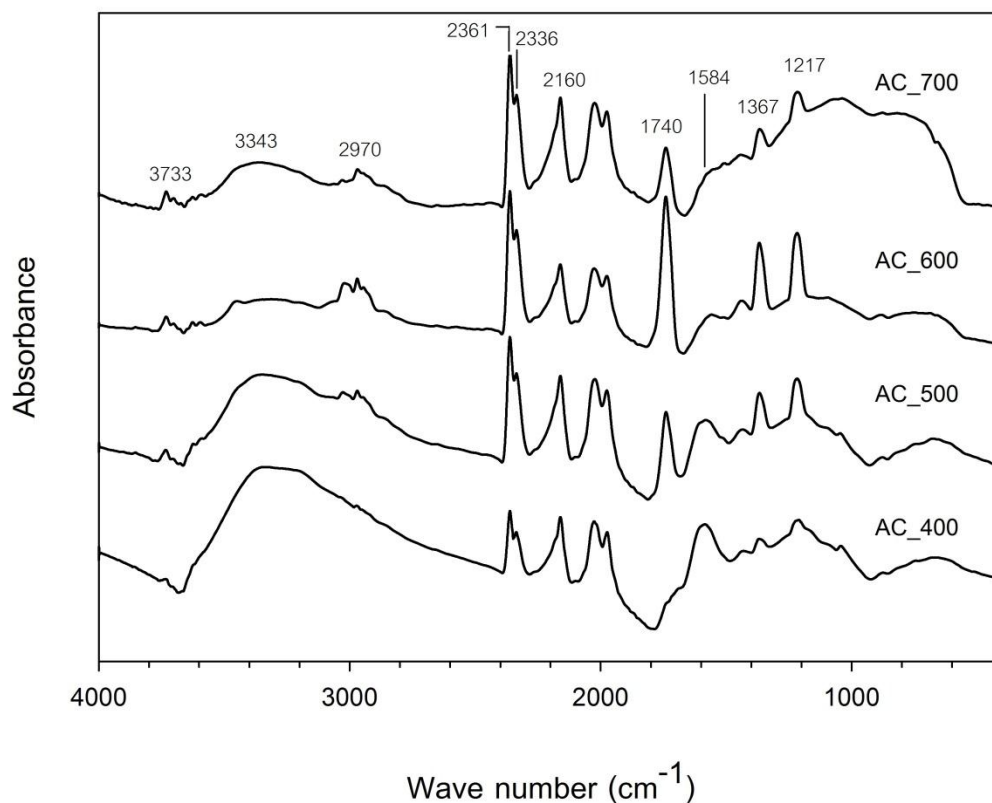


Figure 5.4 FT IR spectra of activated carbon catalysts

The FT-IR spectra are the common technique to analyze the chemical structure of activated carbon as surface oxygen functional groups. Figure 5.4 displays FT-IR spectra of activated carbon derived from deoiled rice bran with different activation temperatures.

All catalysts show band in range of 2900-3700  $\text{cm}^{-1}$ . The broad band located around 3343  $\text{cm}^{-1}$  could be attributed to the O-H stretching vibration of hydroxyl group as alcohols and phenol or/and hydrogen bonded-OH group as water molecule. The band at 2970  $\text{cm}^{-1}$  is related to C-H interaction with carbon surface. The sharp bands located at 2361, 2336 and 2160  $\text{cm}^{-1}$  are attributed to the  $\text{C}\equiv\text{C}$  stretching vibration of alkyne group. There is the shape band at 1740  $\text{cm}^{-1}$  which can be denoted as stretching C=O of carbonyl groups. Moreover, the band at around 1580 to

$1720\text{ cm}^{-1}$  may be attributed to the C=C stretching vibration of aromatic ring and/or C=O of lactonic and carboxylic group. It is observed that the AC\_400 sample displays obviously sharp band as compared to other catalysts. In region at around  $1367$  and  $1217\text{ cm}^{-1}$  may relate to C–O stretching vibration. In fact, carboxyl, anhydride and lactone are acidic, while phenol, carbonyl, quinine and ether are neutral or weak acid. Consequently, the presence of oxygen surface functional group may be associated with the total acidity. It appears that the result from IR spectra consistent with total acid density obtained using standard acid-base back titration [2, 35, 36].



### 5.1.7 Catalytic activity of activated carbon catalysts for ethanol dehydrogenation

The catalytic activity of activated carbon catalysts has been examined in the dehydrogenation of ethanol at various reaction temperatures.

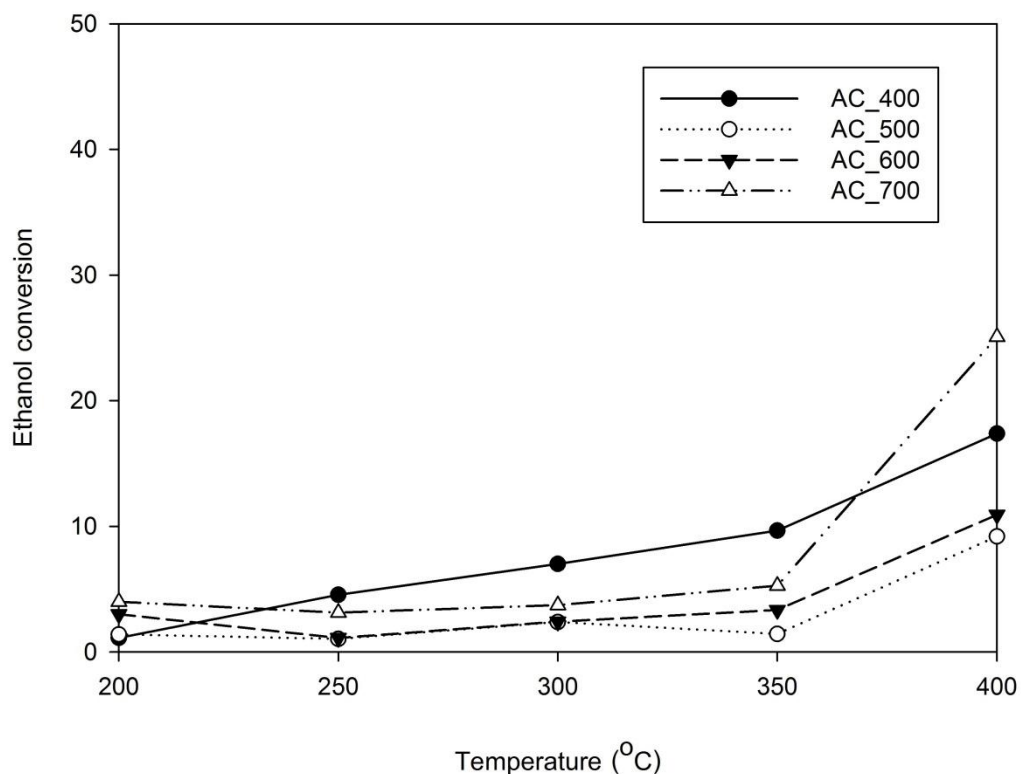


Figure 5.5 Conversion of ethanol as a function of reaction temperature using activated carbon catalysts

Figure 5.5 represents the steady state conversion of ethanol on the activated carbon catalysts derived from deoiled rice bran with different activation temperatures. As expected, ethanol conversion increases with increasing the reaction temperature because of its endothermic reaction. At low temperature (200-350°C), it is obviously seen that the AC\_400 catalyst shows the highest activity among other catalysts. Especially at temperature of 350°C, the AC\_400 catalyst shows ethanol conversion about 10% while other catalysts (AC\_500, AC\_600 and AC\_700) display similar ethanol conversion which was achieved less than 5%. Consequently, it concluded that the

highest ethanol conversion is obtained with the AC\_400 catalyst even though the conversion with AC\_700 catalyst is much higher than the AC\_400 catalyst at high temperature (400°C). According to previous result, the AC\_400 catalyst has the highest total acid density ( $0.720 \mu\text{mol}/\text{m}^2$ ). Therefore, it may be summarized that the conversion reactions of ethanol was dependent on total acid density. The result agrees with report of Carrasco-Marin F. et al. [6] who reported that ethanol conversion increased with rise in the total surface acidity of carbon catalysts prepared by oxidizing treatment with  $(\text{NH}_4)_2\text{S}_2\text{O}_8$ . In addition, the increasing of amount of sulfur (measured by XRF analysis) may be the minor cause of decreasing ethanol conversion.

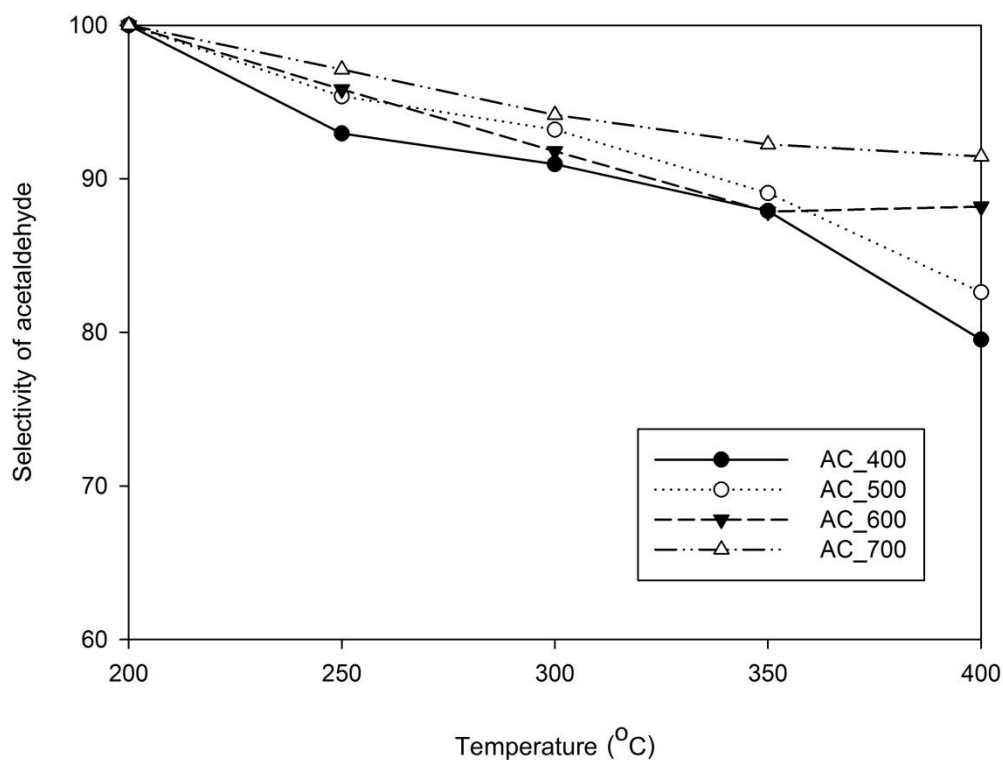


Figure 5.6 Selectivity of acetaldehyde as a function of reaction temperature using activated carbon catalysts

The selectivity (in mol %) is defined as the molar ratio of a specific product to main products (ethylene, acetaldehyde and di-ethyl ether) formed. As shown in Figure 5.6, acetaldehyde selectivity of all catalysts slightly decreases with rising in the reaction temperature. It also represents clearly that the AC\_700 catalyst which has

high amount of zinc, shows the highest selectivity of acetaldehyde. At the highest reaction temperature ( $400^{\circ}\text{C}$ ), the AC\_700 catalyst, showed selectivity of acetaldehyde as high as approximately 91%. While the AC\_400 catalyst which has the lowest amount of zinc, shows the lowest selectivity of acetaldehyde as about 80%. Therefore, it may be presumed that the selectivity of acetaldehyde was dependent on amount of zinc residue.

When considered in term of acetaldehyde yield as shown in Figure 5.7, it is observed that AC\_400 catalyst exhibits the highest yield of acetaldehyde even though the acetaldehyde yield with AC\_700 catalyst is much higher than the AC\_400 catalyst at high temperature. Consequently, it is assumed that total acid density was a major effect on catalytic activity for ethanol dehydrogenation.

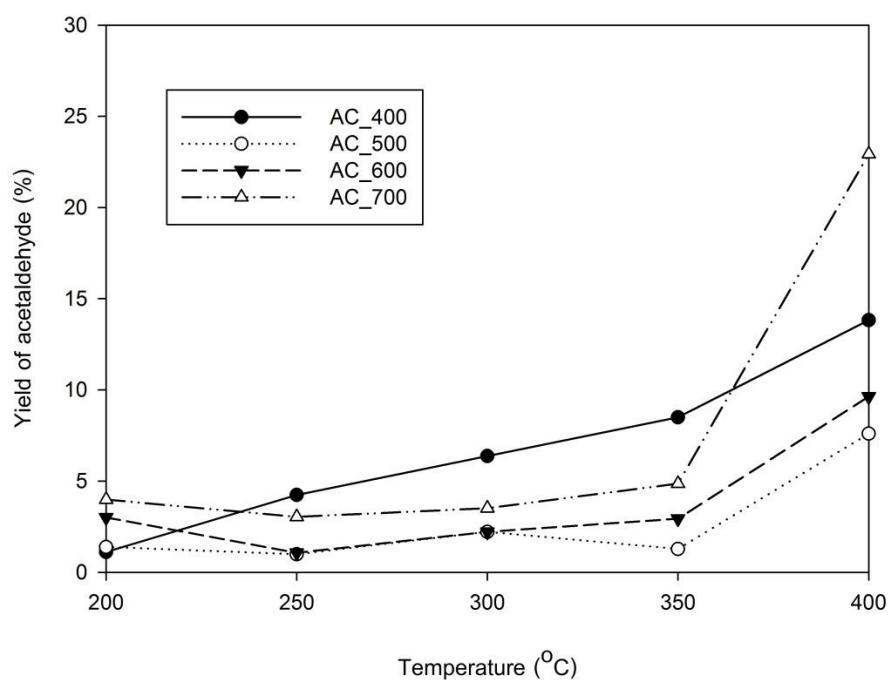


Figure 5.7 Yield of acetaldehyde as a function of reaction temperature using activated carbon catalysts



In addition, the selectivity of ethylene is inverse proportional with the selectivity of acetaldehyde as shown in Figure 5.8 as an example.

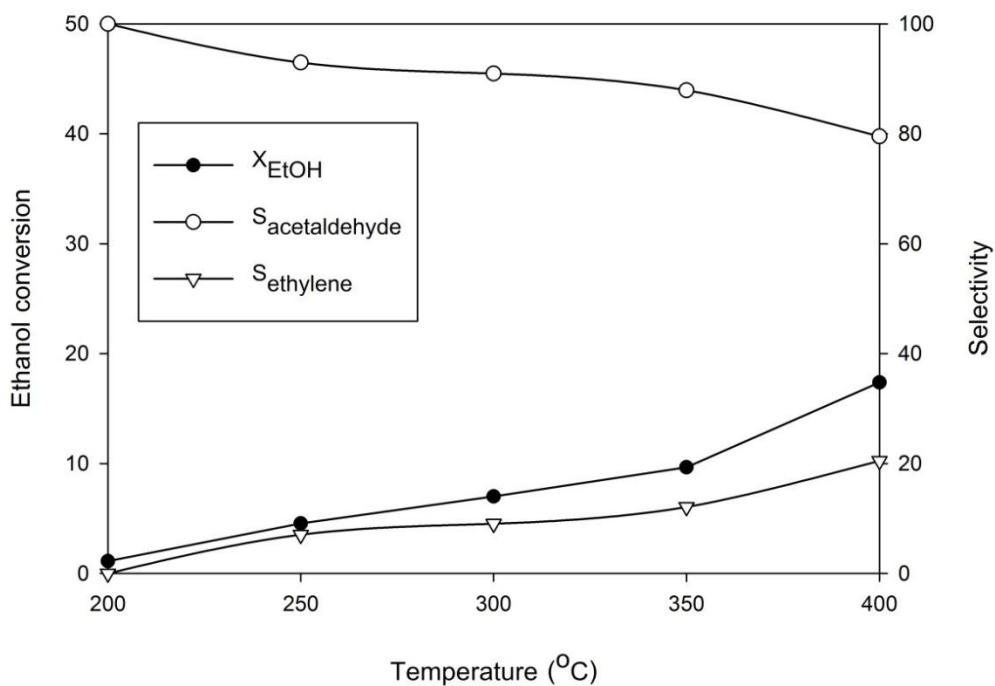


Figure 5.8 Ethanol conversion and selectivity of products as a function of reaction temperature using AC\_400 catalyst

All catalyst is in similar trend for both ethanol conversion and selectivity. Figure 5.8 represents clearly both conversion and selectivity of the AC\_400 catalyst. The main product and byproduct are acetaldehyde and ethylene, respectively. Therefore, it can be summarized that activated carbon derived deoiled rice bran by chemical activation with  $\text{ZnCl}_2$  act mainly as ethanol dehydrogenation catalyst, which produced acetaldehyde as main product.

## 5.2 Characteristics and catalytic activity of nickel catalysts supported on activated carbon for ethanol dehydrogenation

This part describes the characteristic and behavior of nickel catalyst which supported on activated carbon (commercial grade) with various percentage of nickel loading. Moreover, activated carbon derive from deoiled rice bran is also used as support for nickel catalyst to compare the catalytic activity for ethanol dehydrogenation with nickel catalyst supported on the commercial activated carbon.

### 5.2.1 A commercial activated carbon analysis

The metal contaminants of a commercial activated carbon as seen in Table 5.3 were examined by EDX analysis. It was found that the main contaminants are Si and Al element. Moreover, there also has little amount of Cu, Cr, Fe and Ni as transition metal in activated carbon. These contaminants may be able to play a significant role in the catalytic activity for ethanol dehydrogenation.

**Table 5.3 The contaminants of a commercial activated carbon obtained by EDX**

Element	% Weight
Si	35.35
Al	12.83
Cu	10.39
Cr	8.31
Fe	6.83
Ni	6.44
Others (Mg, Ca, K)	≈15

### 5.2.2 Nitrogen physisorption

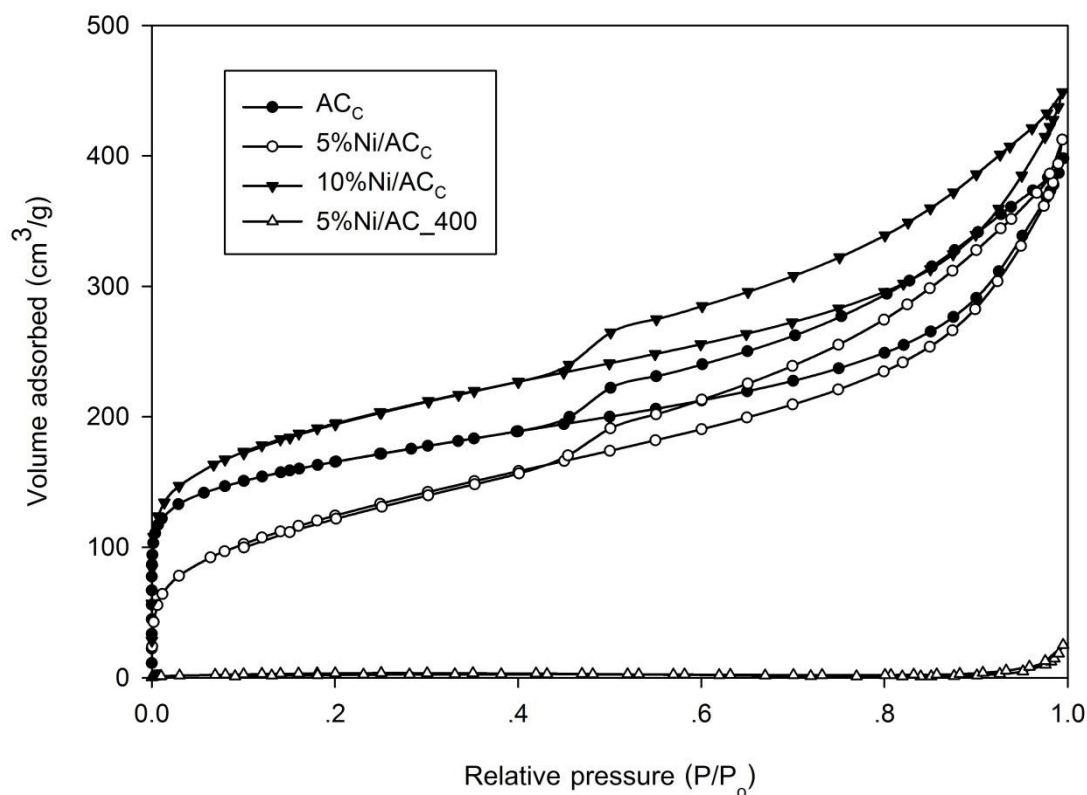


Figure 5.9  $N_2$  adsorption-desorption isotherms at  $-196^\circ\text{C}$  of the nickel catalysts supported on activated carbon

The nitrogen isotherms of commercial activated carbon and nickel catalysts are shown in Figure 5.9. It is observed that the  $AC_C$ ,  $5\%Ni/AC_C$  and  $10\%Ni/AC_C$  catalysts show hysteresis loop at high relative pressure ( $P/P_0 > 0.4$ ). It can be denoted as mesopore structure. In addition, these catalysts also exhibit the  $N_2$  adsorption at low relative pressure ( $P/P_0 < 0.4$ ), indicating the presence of micropore structure. Nevertheless, it is a wide microporous structure which is observed from increasing of the amount of  $N_2$  adsorbed at low relative pressure. For the  $5\%Ni/AC_{400}$  catalyst, there are scarcely any  $N_2$  adsorbed at every relative pressure, which indicating to being non-porous material.

Table 5.4 summarized the porous properties obtained from  $N_2$  adsorption-desorption isotherm. Surface area and micropore volume of the  $AC_C$  catalyst are

approximately  $563 \text{ m}^2/\text{g}$  and  $0.17 \text{ cm}^3/\text{g}$ , respectively. It appears that loading with 5% nickel onto activated carbon used as support (both 5%Ni/AC<sub>C</sub> and 5%Ni/AC<sub>400</sub>) decreases the surface area and pore volume, which could be attributed to the pore blockage by nickel clusters. However, surface area increased with nickel loading as 10% (10%Ni/AC<sub>C</sub> catalyst). Consequently, it is assumed that a higher amount of nickel loading activates the carbon structures, which the narrow porous (new surface) are opened [37].

**Table 5.4 Porous properties of nickel catalysts and commercial activated carbon**

Catalysts	$S_{\text{BET}}$ ( $\text{m}^2/\text{g}$ )	$S_{\text{mic}}$ ( $\text{m}^2/\text{g}$ )	$V_{\text{total}}$ ( $\text{cm}^3/\text{g}$ )	$V_{\text{mic}}$ ( $\text{cm}^3/\text{g}$ )	$D_p$ (nm)
AC <sub>C</sub>	563	353	0.59	0.17	4.18
5%Ni/AC <sub>C</sub>	440	161	0.59	0.09	5.38
10%Ni/AC <sub>C</sub>	665	416	0.65	0.21	4.00
5%Ni/AC <sub>400</sub>	11	-	0.02	-	7.41

$S_{\text{BET}}$  = BET surface area;  $S_{\text{mic}}$  = Micropore area calculated by t-Plot method;

$V_{\text{total}}$  = Total pore volume;  $V_{\text{mic}}$  = Micropore volume;  $D_p$  = Average pore diameter

Pore size distributions of porous materials are shown in Figure 5.10. It is seen that pore size of catalysts is mainly in range of 2-7 nm, which indicates mesoporous type. However, these catalysts also consist of the large mesopore structure (>7 nm).

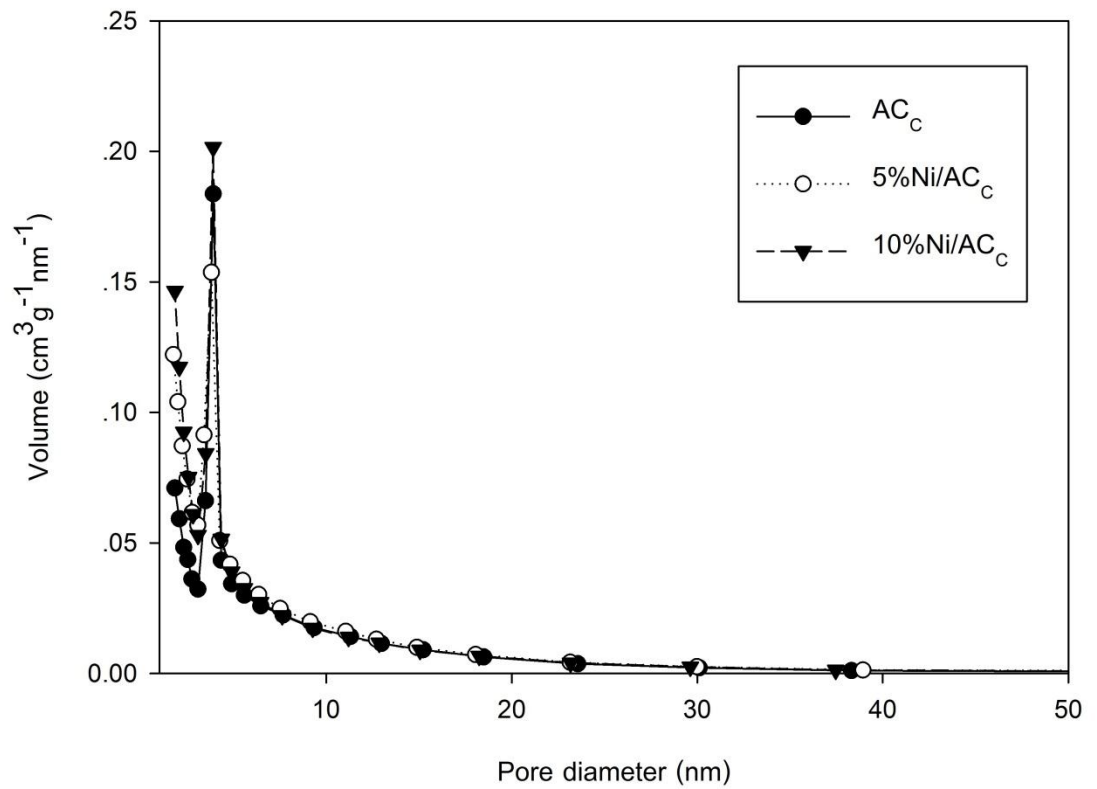


Figure 5.10 BJH pore size distribution for porous carbon catalysts

### 5.2.3 X-ray diffraction (XRD)

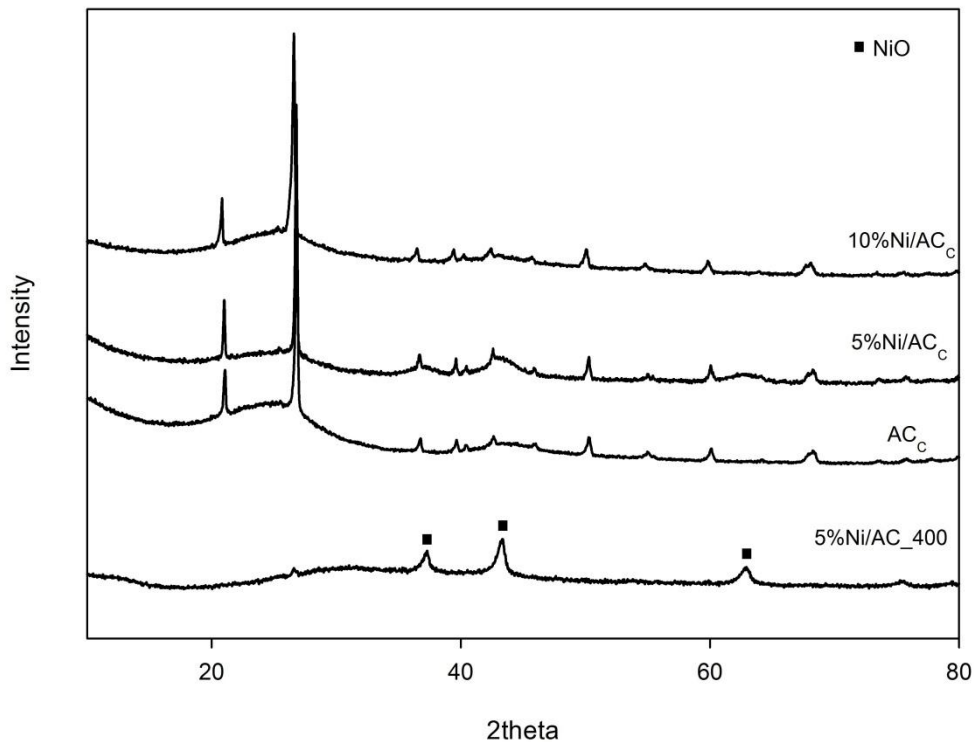


Figure 5.11 XRD patterns of nickel catalysts supported on activated carbon

The XRD patterns of nickel supported on activated carbon are shown in Figure 5.11. The XRD pattern of AC<sub>c</sub> sample used as support exhibits sharp diffraction peak at  $2\theta = 26.8$ , which can be denoted as graphite structure on activated carbon [38]. For nickel catalyst supported on AC<sub>c</sub>, it appears that these XRD pattern is similar with their support. Therefore, it is assumed that nickel loaded onto activated carbon both 5 and 10% loading is well dispersed. For 5%Ni/AC<sub>400</sub> catalyst, the NiO peaks display obviously at  $2\theta = 37.2$ ,  $43.5$  and  $62.8$  [39], indicating the large crystallite size.

#### 5.2.4 Transmission electron microscopy (TEM)

TEM micrographs of nickel catalyst supported on activated carbon by different percentages of nickel loading are shown in Figure 5.12. From TEM micrograph of both 5%Ni/AC<sub>C</sub> and 10%Ni/AC<sub>C</sub>, it was found that nickel species (dark spot) are well dispersion. The average crystallite size of nickel is 6 nm. This result conforms to XRD pattern.

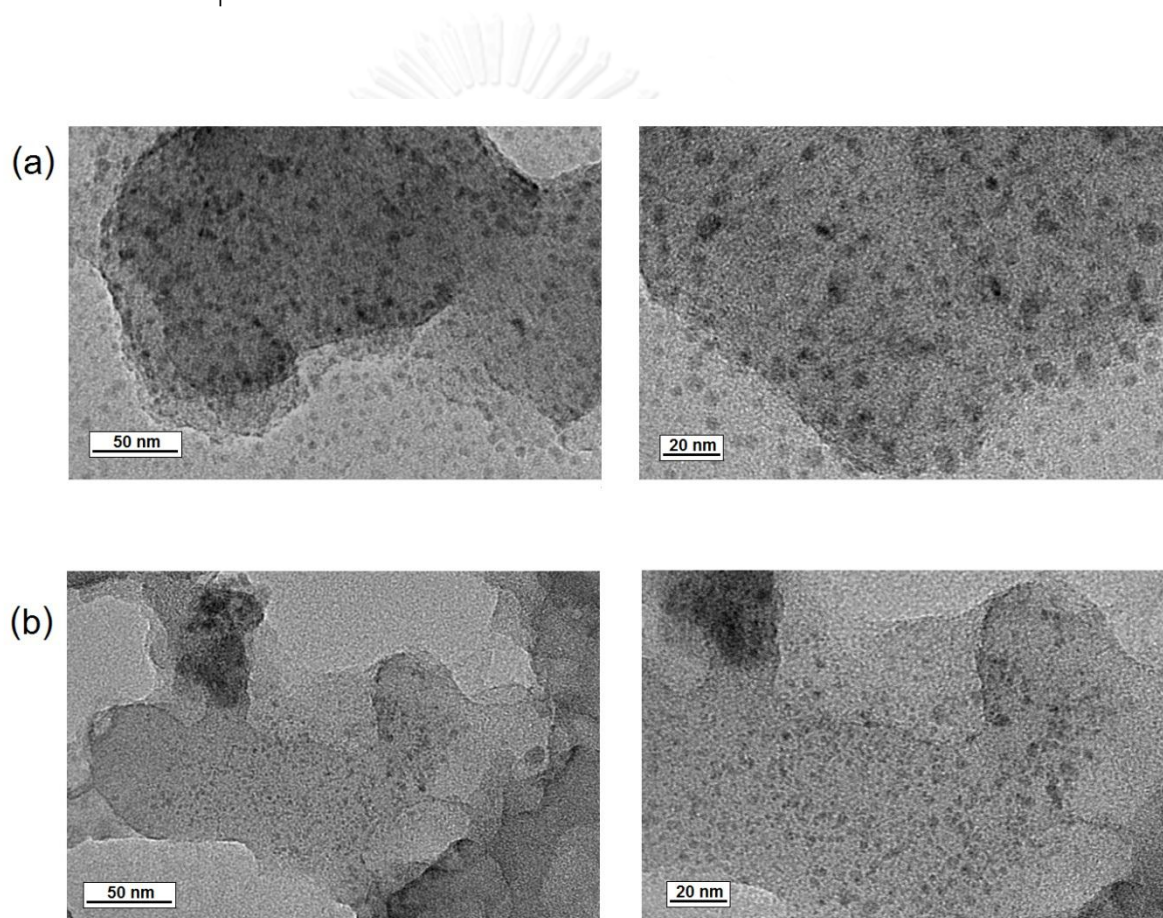


Figure 5.12 TEM micrograph of nickel catalysts supported on activated carbon (a) 5%Ni/AC<sub>C</sub> and (b) 10%Ni/AC<sub>C</sub>



### 5.2.5 Scanning Electron Microscopy (SEM) and Energy dispersive X-ray spectroscopy (EDX)

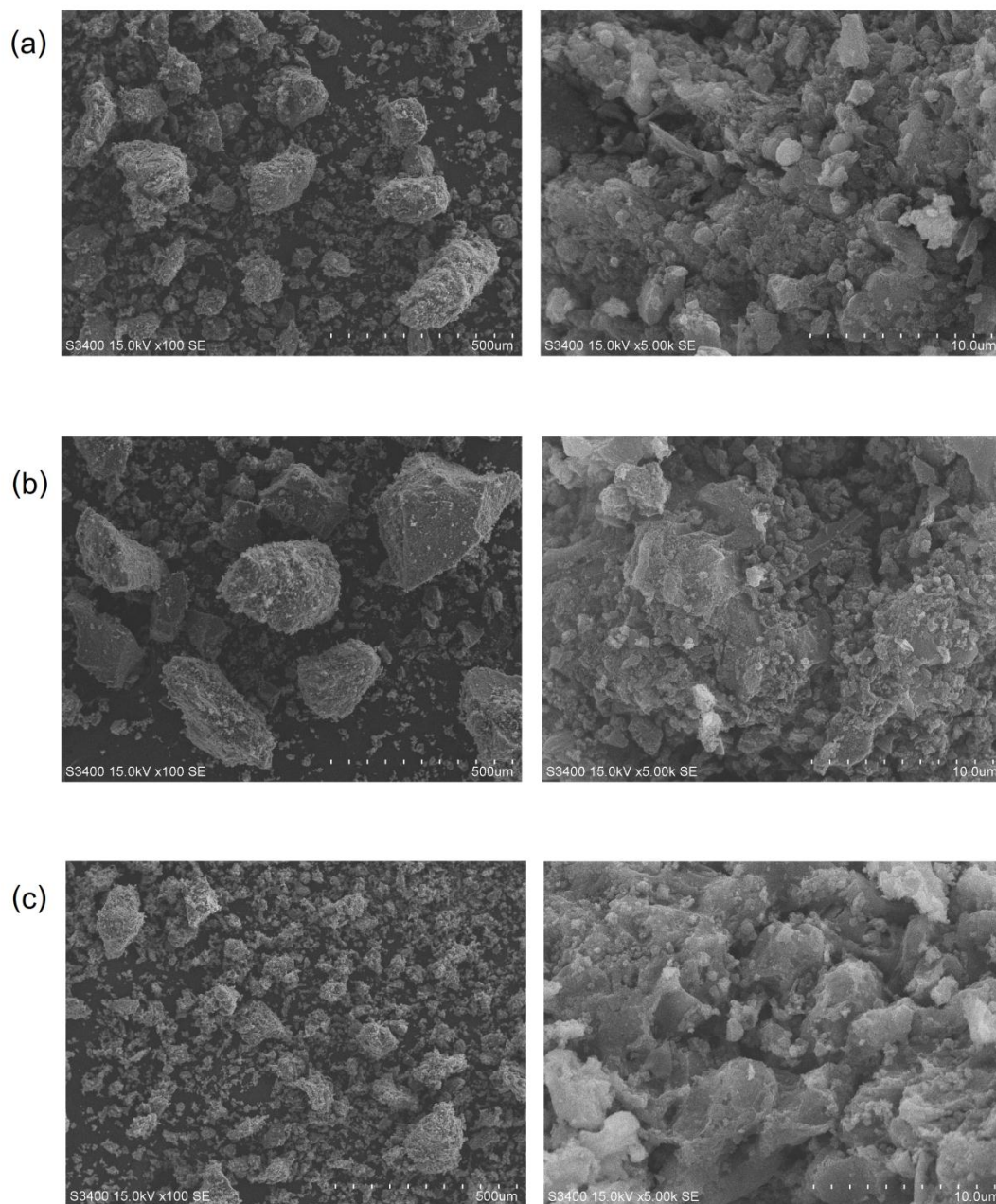


Figure 5.13 SEM micrograph of nickel catalysts supported on activated carbon (a) 5%Ni/AC<sub>C</sub>; (b) 10%Ni/AC<sub>C</sub> and (c) 5%Ni/AC<sub>400</sub>



The morphology and nickel distribution of catalysts obtained from SEM/EDX analysis are shown in Figure 5.13 and 5.14, respectively. From SEM micrograph of both 5%Ni/AC<sub>c</sub> and 10%Ni/AC<sub>c</sub>, it appears the cluster of catalyst particle. Figure 5.14 represents EDX mapping of element distribution of nickel catalysts. It was found that nickel distribution of 5%Ni/AC<sub>c</sub> and 10%Ni/AC<sub>c</sub> catalysts is good, which consistent with result from XRD pattern (as seen in Figure 5.11). The 5%Ni/AC<sub>400</sub> catalyst shows poor dispersion of nickel species on the activated carbon which also corresponding with XRD pattern appeared for NiO peak.

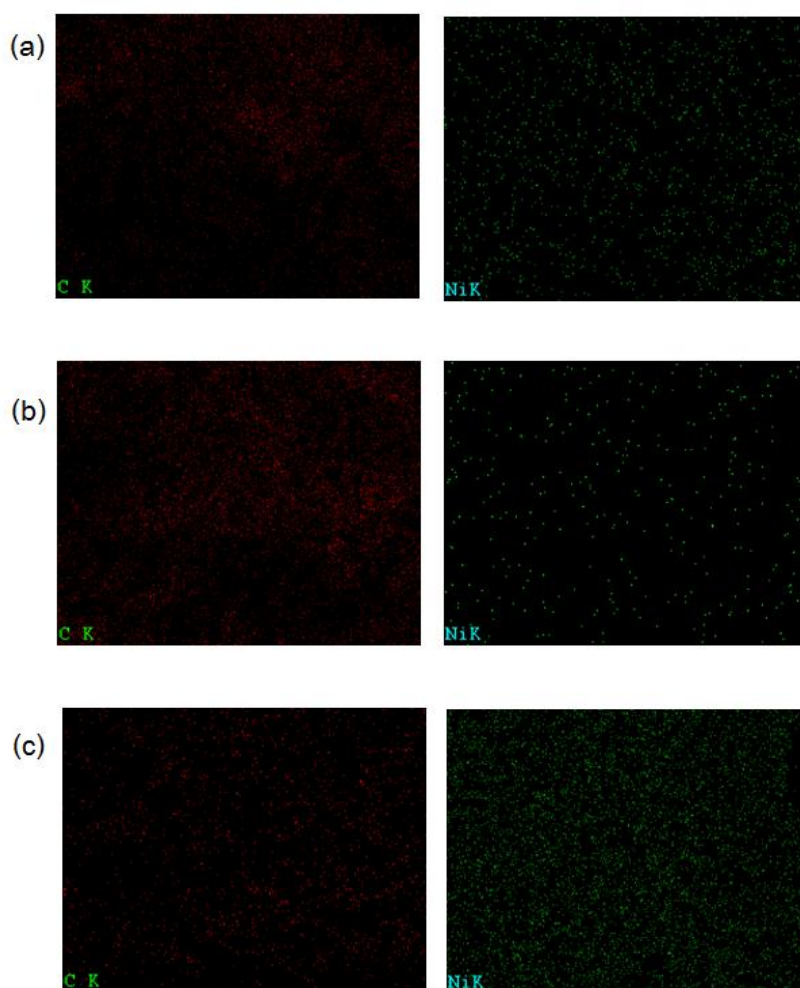


Figure 5.14 EDX mapping of nickel catalysts supported on activated carbon (a) 5%Ni/AC<sub>c</sub>; (b) 10%Ni/AC<sub>c</sub> and (c) 5%Ni/AC<sub>400</sub>

Table 5.5 EDX analysis of nickel catalysts supported on activated carbon

Catalysts	%Weight			%Atomic	
	Ni	C	Ni : C ratio	Ni	C
5%Ni/AC <sub>c</sub>	23.00	77.00	0.30	5.76	94.24
10%Ni/AC <sub>c</sub>	13.49	86.51	0.16	3.09	96.91
5%Ni/AC <sub>400</sub>	68.13	31.87	2.13	30.43	69.57

The percentages of nickel and carbon element of catalysts are shown in Table 5.5. The 5%Ni/AC<sub>c</sub> catalyst shows %weight of nickel is approximately 23.0%, which much higher than the 10%Ni/AC<sub>c</sub> catalyst which has low %weight of nickel as about 13.5%. Conversely, it means that the 5%Ni/AC<sub>c</sub> catalyst has lower %carbon element than 10%Ni/AC<sub>c</sub> catalyst. When considered upon the same %loading of nickel onto different activated carbon (5%Ni/AC<sub>c</sub> compare with 5%Ni/AC<sub>400</sub> catalyst), 5%Ni/AC<sub>400</sub> presents higher %weight of nickel than 5%Ni/AC<sub>c</sub> catalyst, which is related to the lower %weight of carbon.

### 5.2.6 Thermogravimetric and differential thermal analysis (TG/DTA)

Figure 5.15 represents the thermal decomposition of a commercial activated carbon (AC<sub>c</sub>) under nitrogen atmosphere in the temperature range of room temperature to 1000°C. The weight loss occurs at temperature range 50 to 150°C, which indicating the moisture elimination. At temperature range about 200 to 400°C, the weight of commercial activated carbon (AC<sub>c</sub>) slightly decreases. Moreover, the main weight loss occurs at temperature above 400°C which may be attributed to the thermal decomposition of organic molecule. However, a commercial activated carbon (AC<sub>c</sub>) is lower weight loss than the AC<sub>400</sub> sample (as see in Figure 5.3a).

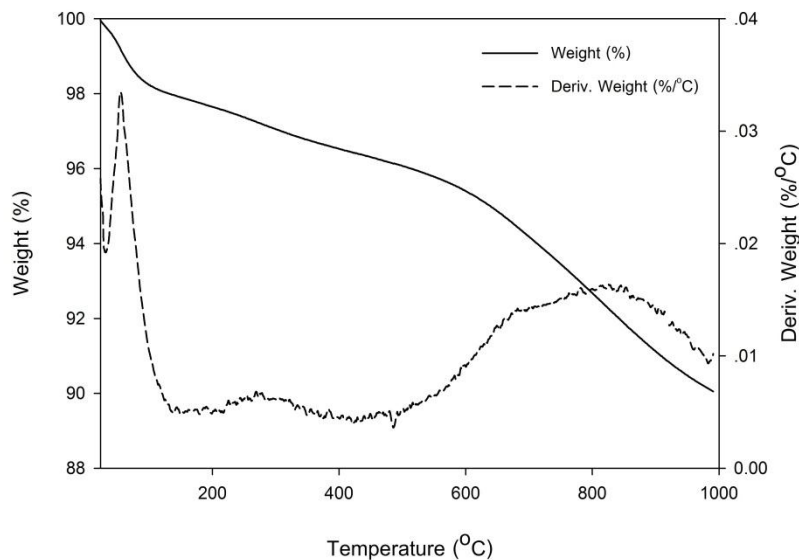


Figure 5.15 Thermal analysis of  $AC_C$  sample under nitrogen atmosphere

To investigate the decomposition of nickel catalysts during the calcination, the thermal decomposition of the catalysts precursor is studied by in situ TGA/DTA analysis under air as shown in Figure 5.16. These catalyst precursors mean activated carbon impregnated with  $Ni(NO_3)_2 \cdot 6H_2O$  as nickel precursor (without calcination) which are denoted as 5%Ni/ $AC_C$ -N, 10%Ni/ $AC_C$ -N and 5%Ni/ $AC_{400}$ -N.

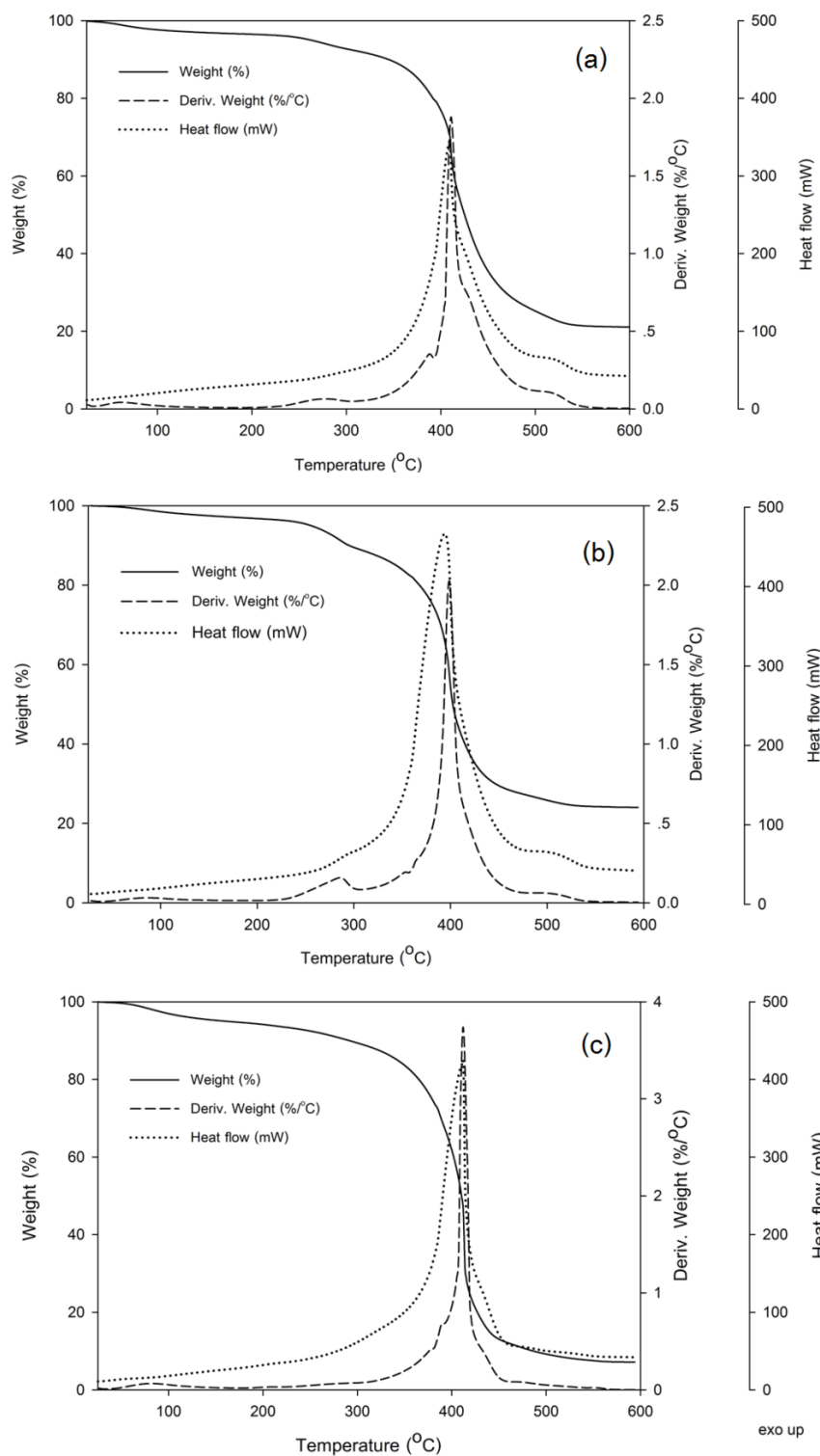


Figure 5.16 in situ TGA/DTG analysis of activated carbon impregnated with  $\text{Ni}(\text{NO}_3)_2 \cdot 6\text{H}_2\text{O}$  (without calcination) under air (a) 5%Ni/AC<sub>C</sub>-N; (b) 10%Ni/AC<sub>C</sub>-N and (c) 5%Ni/AC<sub>400</sub>-N

From Figure 5.16, all samples have little weight loss at temperature around  $100^{\circ}\text{C}$ , indicating the moisture elimination. The weight loss occurred at temperature range of about  $200\text{-}300^{\circ}\text{C}$  is due to the decomposition of nickel nitrate to release  $\text{HNO}_3$  and  $\text{NO}_x$  molecules. Consequently, it is observed clearly that 10%Ni/AC<sub>C</sub>-N sample which consists of higher nitrate molecule, shows higher weight loss at this region than 5%Ni/AC<sub>C</sub>-N and 5%Ni/AC<sub>400</sub>-N. However, the main weight loss occurs at the temperature around  $400^{\circ}\text{C}$ , which may be attributed to decomposition of carbon structure. In fact, carbon is oxidized by oxygen to yield CO and CO<sub>2</sub> as products. As seen in Figure 5.16a and 5.16b, the weight loss at this stage of 5%Ni/AC<sub>C</sub>-N sample is higher than 10%Ni/AC<sub>C</sub>-N sample because of more carbon oxidized. It is presumed that the presence of nitrate molecules from  $\text{Ni}(\text{NO}_3)_2 \cdot 6\text{H}_2\text{O}$  might prevent the oxidation of carbon by oxygen, which is illustrated obviously by Figure 5.17. Therefore, it indicates that 5%Ni/AC<sub>C</sub>-N sample has carbon remained less than 10%Ni/AC<sub>C</sub>-N sample. This result is consistent with EDX analysis.

Moreover, Figure 5.16c represents the in situ TG/DTA analysis of 5%Ni/AC<sub>400</sub>-N sample compared with 5%Ni/AC<sub>C</sub>-N sample when considered at the same %loading of nickel onto different activated carbon. As expected, the weight loss of 5%Ni/AC<sub>400</sub>-N sample is higher than the 5%Ni/AC<sub>C</sub>-N sample. Due to the nature of AC<sub>400</sub> used as support has high weight loss (as seen in figure 5.3a) and/or easier oxidized. Consequently, one of cause of over decreasing of surface area on 5%Ni/AC<sub>400</sub> after calcination with air could be attributed to more carbon destroyed. Its low surface area affects poor nickel dispersion.



### 5.2.7 X-ray photoelectron spectroscopy (XPS)

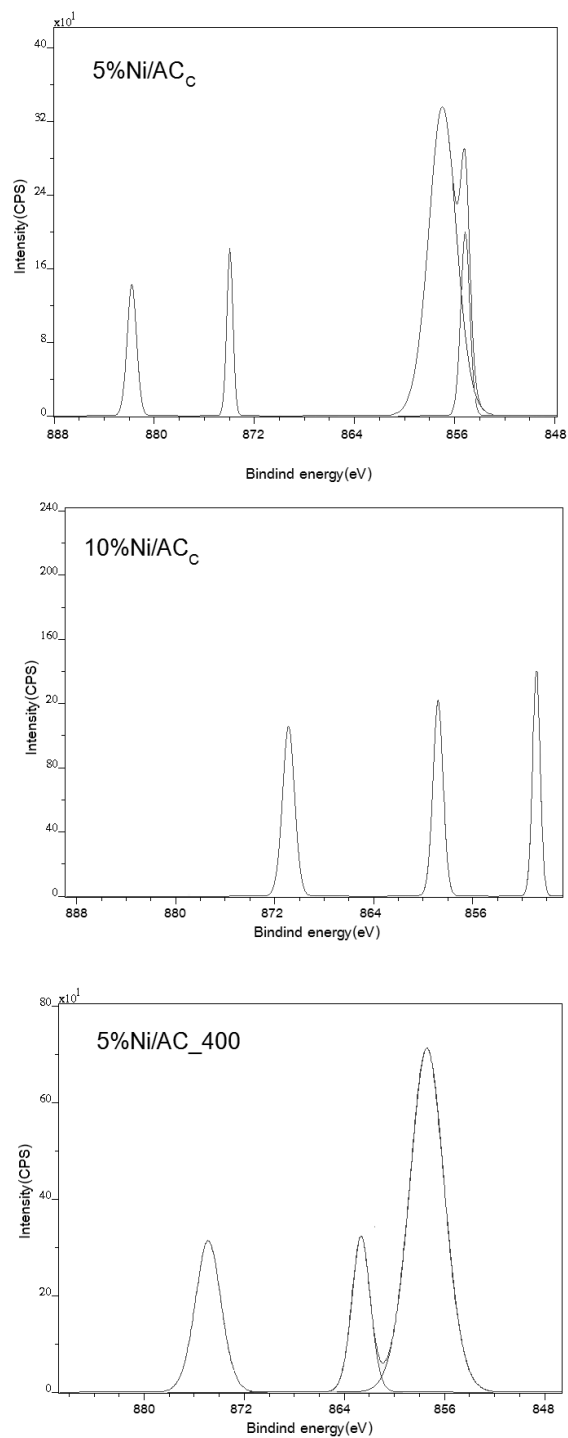


Figure 5.18 The deconvolution of Ni 2p of nickel catalysts from XPS analysis

The deconvoluted XPS spectra of Ni 2*p* of nickel catalysts are shown in Figure 5.18. These spectra are divided into two ranges as follows: Binding energy of 870-885 eV denoted as Ni 2*p*<sub>1/2</sub> and Binding energy of 845-869 eV denoted as Ni 2*p*<sub>3/2</sub>[40]. However, it appears that the main spectrum of all catalysts is Ni 2*p*<sub>3/2</sub>. Table 5.6 summarizes the peak parameter of Ni 2*p*<sub>3/2</sub> calculated from XPS spectra. It was found that the nickel concentration on the surface by XPS analysis corresponds to the result from EDX.

Table 5.6 The peak position FWHM and %mass concentration of Ni 2*p*<sub>3/2</sub>

Catalysts	Binding energy (eV)	FWHM	%mass concentration
5%Ni/AC <sub>C</sub>	857.0	2.538	1.98
10%Ni/AC <sub>C</sub>	858.8	0.931	0.27
5%Ni/AC_400	857.4	3.210	12.71



## 5.2.8 Catalytic activity of nickel catalysts supported on activated carbon for ethanol dehydrogenation

Catalytic activity of nickel catalysts for ethanol dehydrogenation considered in terms of ethanol conversion and products selectivity are shown in Figure 5.19 and Figure 5.20, respectively.

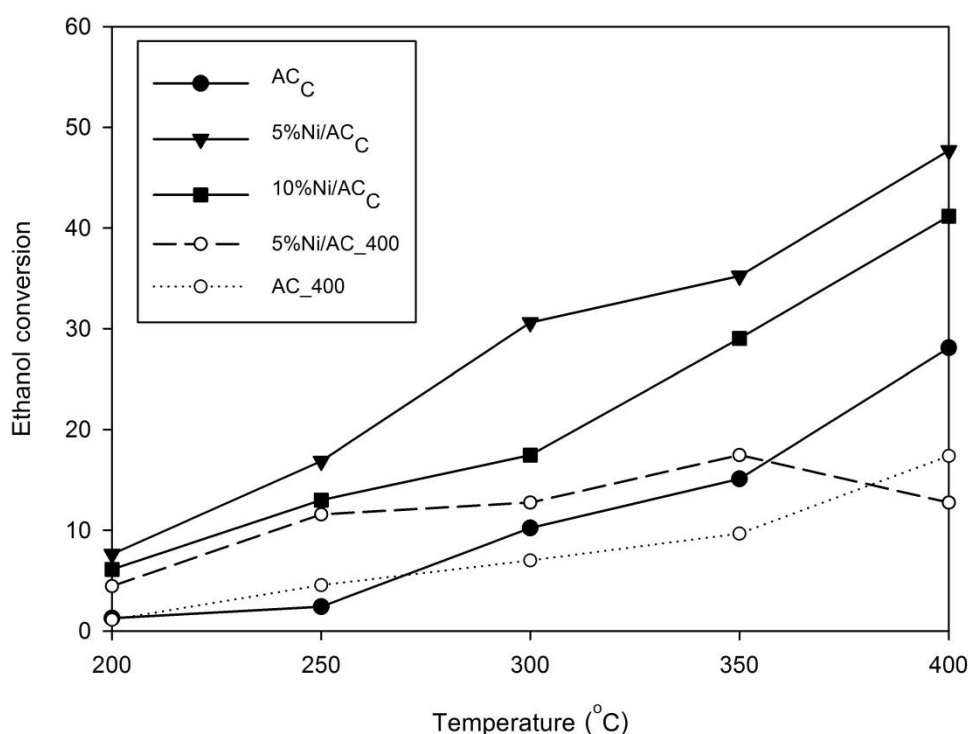


Figure 5.19 Conversion of ethanol as a function of reaction temperature using nickel catalysts

According to Figure 5.19, ethanol conversion in all catalysts increased with rising the reaction temperature from 200 to 400 °C, except for the 5%Ni/AC<sub>400</sub> catalyst that shows maximum conversion at temperature of 350 °C. Figure 5.20 represents selectivity of acetaldehyde and ethylene (as dehydrogenation and dehydration, respectively). All catalysts show that the selectivity of acetaldehyde slightly decreases, while selectivity of ethylene increases with increasing reaction temperature. However, at temperature of 400 °C for all nickel catalysts, selectivity of

acetaldehyde was achieved more than approximately 75%. In addition, there is extremely low selectivity of di-ethyl ether (not shown) as low as approximately 1%.

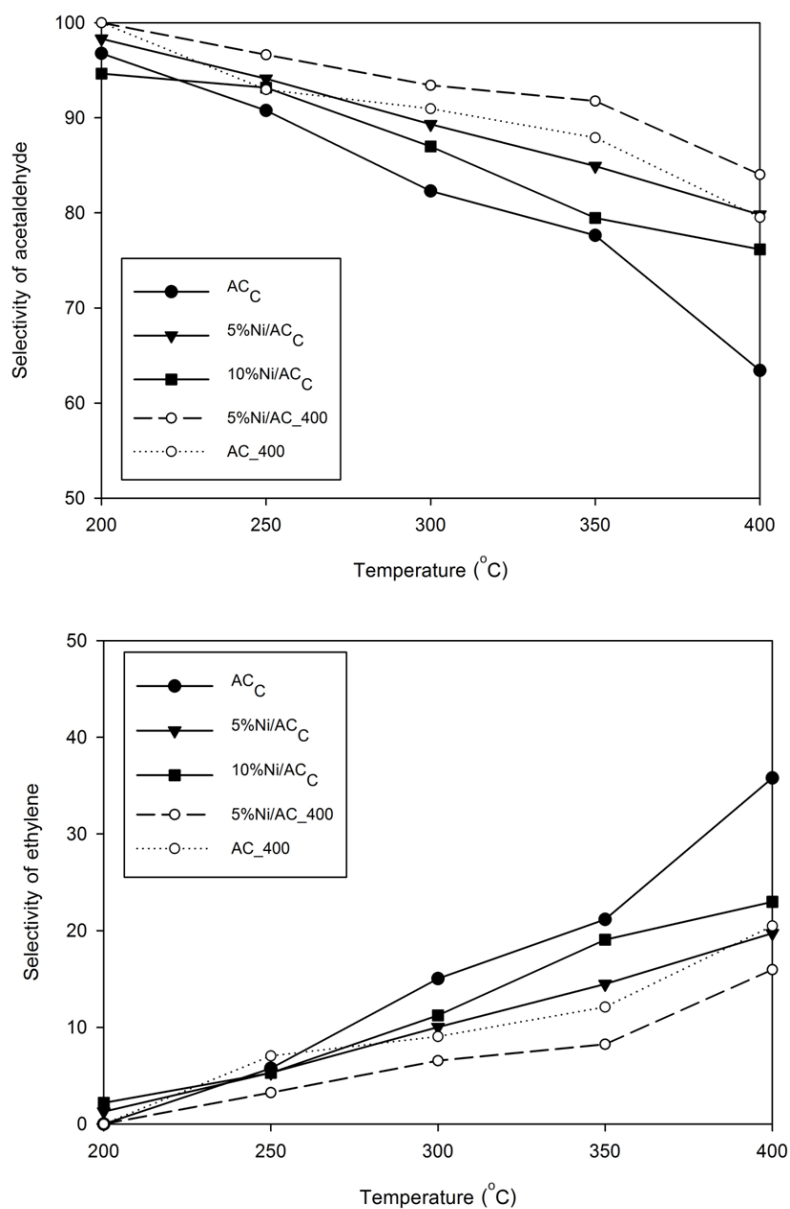


Figure 5.20 Selectivity of products as a function of reaction temperature using nickel catalysts

As seen in Figure 5.19 and Figure 5.20, it appears that loading nickel onto activated carbon increases both ethanol conversion and selectivity of acetaldehyde

as compared to their support. In addition, it was found that 5%Ni/AC<sub>C</sub> catalyst exhibits obviously higher ethanol conversion and selectivity of acetaldehyde than 10%Ni/AC<sub>C</sub> catalyst at every reaction temperature. Due to 5%Ni/AC<sub>C</sub> catalyst shows higher amount of the Ni:C ratio (as observed from EDX and XPS results) than 10%Ni/AC<sub>C</sub> catalyst. Therefore, it may be concluded that catalytic activity for ethanol dehydrogenation toward acetaldehyde is corresponding with the Ni:C ratio. This result shows the similar trend as reported by El-Molla S.A. et al. [22] who found that the activated carbon treated with high loading metal up to 10% decreased the activity of isopropanol dehydrogenation. For the commercial activated carbon (AC<sub>C</sub>), it displays high catalytic activity for ethanol dehydrogenation towards acetaldehyde due to it consists of transition metal as impurities (as shown in Table 5.3). In fact, most transition metal and/or their oxide act as dehydrogenation catalysts.

When considered upon the same %loading of nickel onto different activated carbon (5%Ni/AC<sub>C</sub> compare with 5%Ni/AC<sub>400</sub> catalyst), it was found that 5%Ni/AC<sub>400</sub> catalyst shows lower conversion even though the selectivity of acetaldehyde is higher than 5%Ni/AC<sub>C</sub> catalyst. This result might be attributed to aggregation of nickel to large crystalline.

## CHAPTER 6

### CONCLUSIONS AND RECOMMENDATIONS

#### 6.1 Conclusions

##### 6.1.1 Characteristics and catalytic activity of activated carbon derived deoiled rice bran for ethanol dehydrogenation

This study reports the characteristic and catalytic activity on ethanol dehydrogenation of activated carbons derived deoiled rice bran prepared with different activation temperatures. The results of the study are summarized as following:

- (1) These activated carbons are presented of both microporous and mesoporous.
- (2) The AC\_400 catalyst exhibits the highest surface area and total pore volume, which are  $1404 \text{ m}^2/\text{g}$  and  $0.746 \text{ cm}^3/\text{g}$ , respectively.
- (3) All activated carbons act mainly as ethanol dehydrogenation catalyst, which produced acetaldehyde as the main product.
- (4) The AC\_400 catalyst shows the highest activity among other catalysts due to its highest total acid density.
- (5) Amount of zinc residue from preparation of activated carbon by chemical activation with  $\text{ZnCl}_2$  affects the selectivity of acetaldehyde.

##### 6.1.1 Characteristics and catalytic activity of nickel catalysts supported on activated carbon for ethanol dehydrogenation

This study reports catalytic performance of nickel catalyst supported on commercial activated carbon with different percentages of nickel loading for ethanol dehydrogenation. It also compared with the nickel catalyst supported on AC\_400.

- (1) Nickel distribution on the commercial activated carbon was good.
- (2) Loading nickel onto activated carbon increases the catalytic activity for ethanol dehydrogenation towards acetaldehyde.
- (3) 5%Ni/AC<sub>C</sub> catalyst exhibits obviously higher ethanol conversion and selectivity of acetaldehyde than 10%Ni/AC<sub>C</sub> catalyst due to 5%Ni/AC<sub>C</sub> has higher the amount of the Ni:C ratio than the former.
- (4) 5%Ni/AC<sub>400</sub> catalyst exhibits lower conversion than 5%Ni/AC<sub>C</sub> catalyst, which might be attributed to the aggregation of nickel into large crystalline on 5%Ni/AC<sub>400</sub> catalyst.

## 6.2 Recommendations

- (1) The crystallite size of nickel on activated carbon derived deoiled rice bran should also be investigated by TEM (Transmission electron microscopy) to confirm the XRD result.
- (2) The H<sub>2</sub>-chemisorption analysis should be used to calculate the percentage of dispersion nickel as active site.
- (3) The effect of zinc addition on activated carbon catalysts should be studied on catalytic activity for ethanol dehydrogenation.
- (4) To increase the catalytic performance of activated carbon derived deoiled rice bran, sulfur (remained from preparation activated carbon) as impurity should be removed by new method.
- (5) Deactivation of the catalysts at different reaction temperature should also be investigated in order to improve these catalysts for utilization in industry.

## REFERENCES

1. Niticharoenwong, B., et al., *CHARACTERISTICS OF ACTIVATED CARBONS DERIVED FROM DEOILED RICE BRAN RESIDUES*. Chemical Engineering Communications, 2013. 200(10): p. 1309-1321.
2. Marsh, H. and F.R. Reinoso, *Activated Carbon*. 1 ed. 2006: Elsevier Science. 554.
3. Monser, L. and N. Adhoum, *Modified activated carbon for the removal of copper, zinc, chromium and cyanide from wastewater*. Separation and purification technology, 2002. 26(2): p. 137-146.
4. Sircar, S., T. Golden, and M. Rao, *Activated carbon for gas separation and storage*. Carbon, 1996. 34(1): p. 1-12.
5. Bedia, J., et al., *Preparation and characterization of carbon based acid catalysts for the dehydration of 2-propanol*. Carbon, 2009. 47(1): p. 286-294.
6. Carrasco-Marin, F., A. Mueden, and C. Moreno-Castilla, *Surface-treated activated carbons as catalysts for the dehydration and dehydrogenation reactions of ethanol*. The Journal of Physical Chemistry B, 1998. 102(46): p. 9239-9244.
7. Bedia, J., et al., *Ethanol dehydration to ethylene on acid carbon catalysts*. Applied Catalysis B: Environmental, 2011. 103(3-4): p. 302-310.
8. Neramittagapong, A., W. Attaphaiboon, and S. Neramittagapong, *Acetaldehyde Production from Ethanol over Ni-Based Catalysts*. Science Faculty of Chiang Mai University, 2008. 35(1): p. 171 - 177.
9. W., P.J., *Porosity in Carbons: Characterization and Applications*. 1995: Edward Arnold.
10. Kitano, M., et al., *Preparation of a Sulfonated Porous Carbon Catalyst with High Specific Surface Area*. Catalysis Letters, 2009. 131(1-2): p. 242-249.
11. Montes-Morán, M.A., et al., *On the nature of basic sites on carbon surfaces: an overview*. Carbon, 2004. 42(7): p. 1219-1225.
12. Auer, E., et al., *Carbons as supports for industrial precious metal catalysts*. Applied Catalysis A: General, 1998. 173(2): p. 259-271.
13. Hudlicky, M., *Oxidations in Organic Chemistry*. 1990, Washington, DC.: American Chemical Society.
14. Fieser, L.F. and M. Fieser., *Basic organic chemistry*. 1959, Boston: D.C.: Health and Company.

15. Chang, F.-W., W.-Y. Kuo, and K.-C. Lee, *Dehydrogenation of ethanol over copper catalysts on rice husk ash prepared by incipient wetness impregnation*. Applied Catalysis A: General, 2003. 246(2): p. 253-264.
16. Zhang, M. and Y. Yu, *Dehydration of Ethanol to Ethylene*. Industrial & Engineering Chemistry Research, 2013. 52(28): p. 9505-9514.
17. Fan, D., D.-J. Dai, and H.-S. Wu, *Ethylene Formation by Catalytic Dehydration of Ethanol with Industrial Considerations*. Materials, 2012. 6(1): p. 101-115.
18. Olivares-Marín, M., et al., *Preparation of activated carbon from cherry stones by chemical activation with ZnCl<sub>2</sub>*. Applied Surface Science, 2006. 252(17): p. 5967-5971.
19. Uçar, S., et al., *Preparation and characterization of activated carbon produced from pomegranate seeds by ZnCl<sub>2</sub> activation*. Applied Surface Science, 2009. 255(21): p. 8890-8896.
20. Figueiredo, J.L., et al., *Characterization of active sites on carbon catalysts*. Industrial & engineering chemistry research, 2007. 46(12): p. 4110-4115.
21. Sato, S., et al., *Influence of activated carbon surface acidity on adsorption of heavy metal ions and aromatics from aqueous solution*. Applied Surface Science, 2007. 253(20): p. 8554-8559.
22. El-Molla, S.A., G.A. El-Shobaky, and S.A. Sayed Ahmed, *Catalytic Promotion of Activated carbon by Treatment with Some Transition Metal Cations*. Chinese Journal of Catalysis, 2007. 28(7): p. 611-616.
23. Chang, F.-W., et al., *Ethanol dehydrogenation over copper catalysts on rice husk ash prepared by ion exchange*. Applied Catalysis A: General, 2006. 304: p. 30-39.
24. Badlani, M. and I.E. Wachs, *Methanol: a "smart" chemical probe molecule*. Catalysis Letters, 2001. 75(3-4): p. 137-149.
25. Moreno-Castilla, C., et al., *Dehydration of methanol to dimethyl ether catalyzed by oxidized activated carbons with varying surface acidic character*. Carbon, 2001. 39(6): p. 869-875.
26. Jasinska, E., B. Krzyzyska, and M. Kozłowski, *Activated Carbon Modified with Different Chemical Agents as a Catalyst in the Dehydration and Dehydrogenation of Isopropanol*. Catalysis Letters, 2008. 125(1-2): p. 145-153.
27. Szymanski, G.S. and G. Rychlicki, *Catalytic conversion of propan-2-ol on carbon catalysts*. Carbon, 1993. 31(2): p. 247-257.
28. Bedia, J., et al., *Isopropanol decomposition on carbon based acid and basic catalysts*. Catalysis Today, 2010. 158(1-2): p. 89-96.

29. Bradford, M.C. and M.A. Vannice, *Catalytic reforming of methane with carbon dioxide over nickel catalysts II. Reaction kinetics*. Applied Catalysis A: General, 1996. 142(1): p. 97-122.
30. Wang, S. and G. Lu, *Effects of acidic treatments on the pore and surface properties of Ni catalyst supported on activated carbon*. Carbon, 1998. 36(3): p. 283-292.
31. Zielinski, M., et al., *Hydrogen storage on nickel catalysts supported on amorphous activated carbon*. Catalysis Communications, 2005. 6(12): p. 777-783.
32. Yorgun, S., N. Vural, and H. Demiral, *Preparation of high-surface area activated carbons from Paulownia wood by ZnCl<sub>2</sub> activation*. Microporous and Mesoporous Materials, 2009. 122(1-3): p. 189-194.
33. Shrestha, R., et al., *Preparation and Characterization of Activated Carbon from Lapsi (Choerospondias axillaris) Seed Stone by Chemical Activation with Phosphoric acid*. Research Journal of Chemical Sciences, 2012. 2(10): p. 80-86.
34. Li, W., et al., *Effects of carbonization temperatures on characteristics of porosity in coconut shell chars and activated carbons derived from carbonized coconut shell chars*. Industrial Crops and Products, 2008. 28(2): p. 190-198.
35. Lua, A.C. and T. Yang, *Effect of activation temperature on the textural and chemical properties of potassium hydroxide activated carbon prepared from pistachio-nut shell*. J Colloid Interface Sci, 2004. 274(2): p. 594-601.
36. Tsai, W., et al., *Adsorption of acid dye onto activated carbons prepared from agricultural waste bagasse by ZnCl<sub>2</sub> activation*. Chemosphere, 2001. 45(1): p. 51-58.
37. Mehandjiev, D., E. Bekyarova, and M. Khristova, *Study of Ni-impregnated active carbon*. Journal of colloid and interface science, 1997. 192(2): p. 440-446.
38. Sun, G., et al., *Preparation and characterization of graphite nanosheets from detonation technique*. Materials Letters, 2008. 62(4-5): p. 703-706.
39. Grzechowiak, J.R., I. Szyszka, and A. Masalska, *Effect of TiO<sub>2</sub> content and method of titania-silica preparation on the nature of oxidic nickel phases and their activity in aromatic hydrogenation*. Catalysis Today, 2008. 137(2-4): p. 433-438.
40. Biju, V., *Ni 2p X-ray photoelectron spectroscopy study of nanostructured nickel oxide*. Materials Research Bulletin, 2007. 42(5): p. 791-796.





APPENDICES

จุฬาลงกรณ์มหาวิทยาลัย  
**CHULALONGKORN UNIVERSITY**

## APPENDIX A

### CALCULATION FOR CATALYST PREPARATION

Calculation for preparation of nickel catalyst supported on activated carbon by the incipient impregnation method

Example for 5%Ni/AC<sub>c</sub> catalyst

Based on 1.00 g of catalyst used, the composition of catalyst will be as follow:

$$\text{Nickel} = 0.05 \text{ g}$$

$$\text{A commercial activated carbon} = 1.00 - 0.05 = 0.95 \text{ g}$$

Nickel 0.05 g was prepared from Nickel(II) nitrate hexahydrate

(formula:  $\text{Ni}(\text{NO}_3)_2 \cdot 6\text{H}_2\text{O}$  )

$$\text{Nickel (II) nitrate hexahydrate required} = \frac{\text{MW of Ni}(\text{NO}_3)_2 \cdot 6\text{H}_2\text{O} \times \text{nickel required}}{\text{MW of Ni}}$$

Where Molecular weight of  $\text{Ni}(\text{NO}_3)_2 \cdot 6\text{H}_2\text{O} = 290.79 \text{ g/mol}$  and

Atomic weight of Ni = 58.69 g/mol

$$\begin{aligned} \text{So, Nickel (II) nitrate hexahydrate required} &= \frac{290.79 \times 0.05}{58.69} \\ &= 0.247 \text{ g} \end{aligned}$$

## APPENDIX B

### CALIBRATION CURVES

This appendix showed the calibration curves for calculation of composition of reactant and products in ethanol dehydrogenation reaction. The reactant is ethanol and the main product is acetaldehyde. The other products are ethylene and di-ethyl ether.

The VZ10 column is used with a gas chromatography equipped with a flame ionization detector, Shimadzu model 14B, to analyze the concentration of products including of ethanol, acetaldehyde, ethylene and di-ethyl ether. Conditions used in GC are illustrated in Table D.1.

**Table D.1 Conditions used in Shimadzu model GC-14B**

Parameters	condition
Width	5
Slope	50
Drift	0
Min. area	300
T.DBL	0
Stop time	10
Atten	2
Speed	3
Method	1
Format	1
SPL.WT	100
ID.WT	1

Mole of reagent in y-axis and area reported by gas chromatography in x-axis are showed in the curves. The calibration curves of ethanol, acetaldehyde, ethylene and di-ethyl ether are illustrated in the following figures.

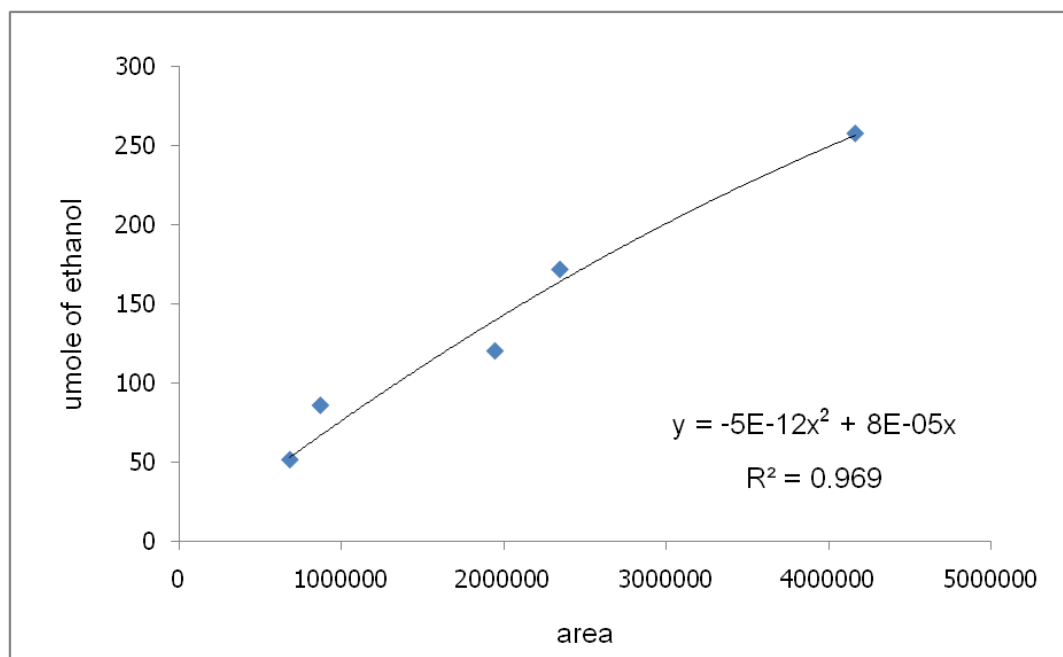


Figure D.1 The calibration curve of ethanol

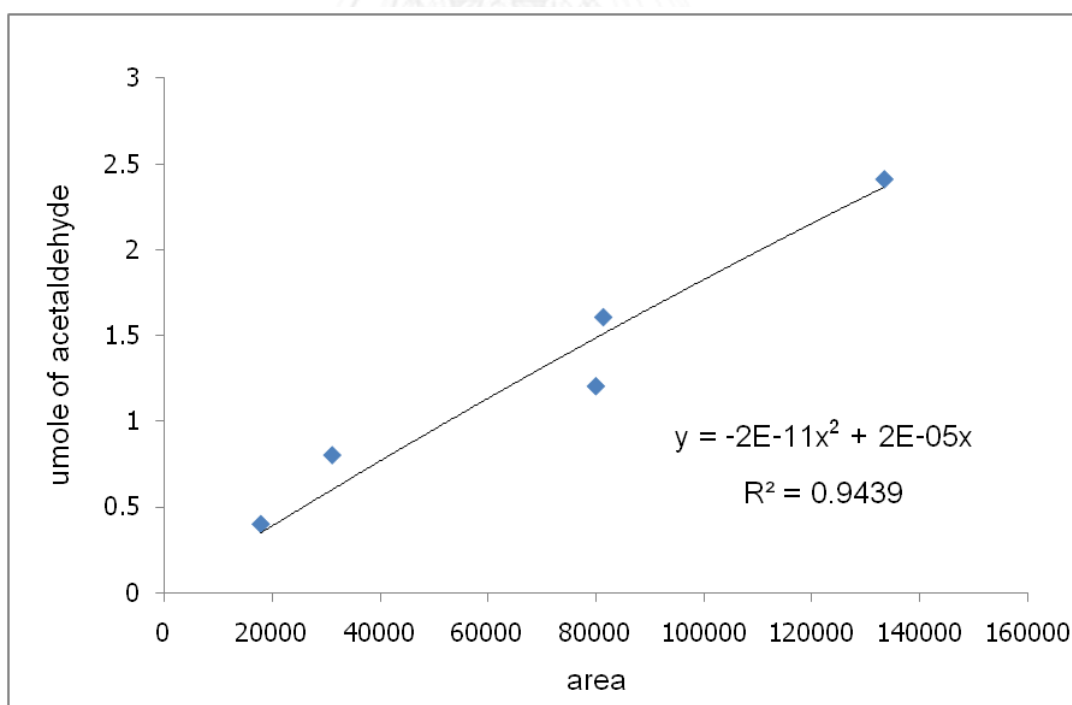


Figure D.2 The calibration curve of acetaldehyde

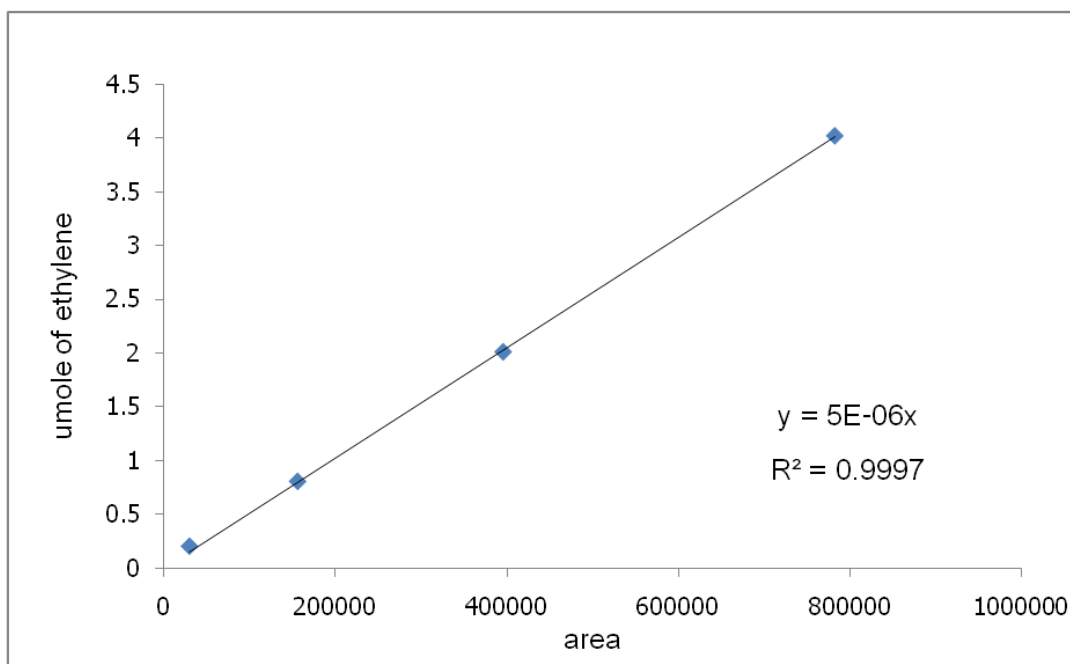


Figure D.3 The calibration curve of ethylene

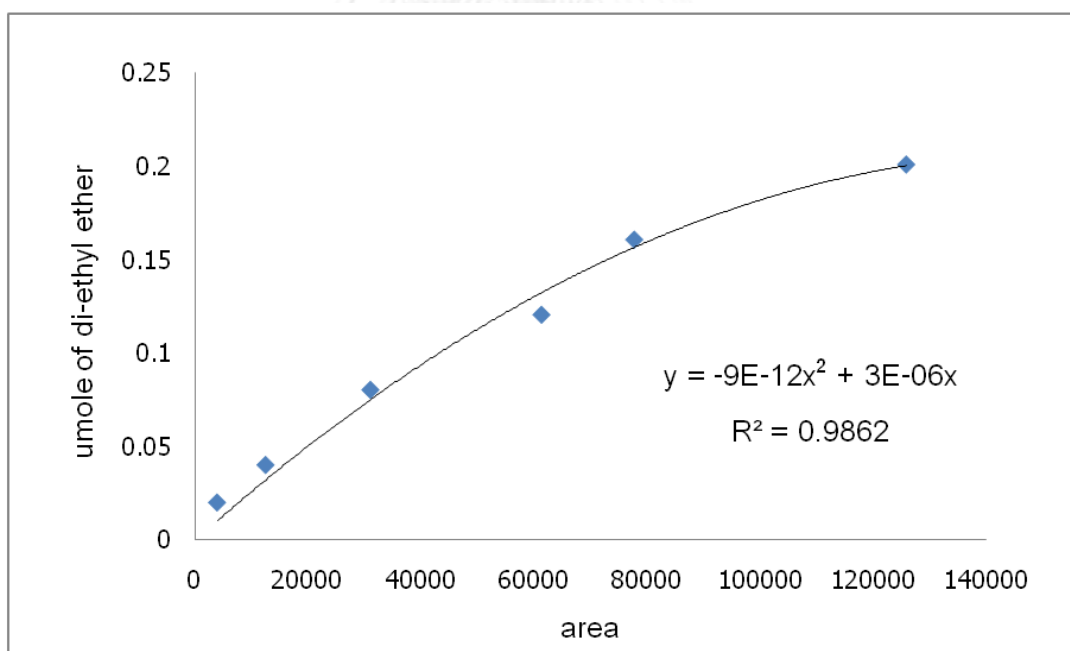


Figure D.4 The calibration curve of di-ethyl ether

## APPENDIX C

### CALCULATION OF ETHANOL CONVERSION AND SELECTIVITY

The catalyst performance for the ethanol dehydrogenation was considered in term of ethanol conversion and selectivity of products.

Ethanol conversion is defined as moles of ethanol converted with respect to ethanol in feed:

$$\text{Ethanol conversion (\%)} = \frac{\text{mole of ethanol in feed} - \text{mole of ethanol in product}}{\text{mole of ethanol in feed}} \times 100$$

Selectivity of product is defined as the molar ratio of a specific product to main products (acetaldehyde, ethylene and di-ethyl ether) formed:

$$\text{Selectivity of B (\%)} = \frac{\text{mole of B formed}}{\text{mole of total main products}} \times 100$$

Where B is product, mole of B formed can be calculated by using calibration curve of product B

$$\text{Yield of B (\%)} = \text{Ethanol conversion} \times \text{Selectivity of B}$$

## VITA

Miss Somrudee Chatchawanrat was born on 18th January 1990, in Nakhonsithammarat, Thailand. She received the Bachelor's degree of Chemical Technology from Faculty of Science, Chulalongkorn University, Thailand in May 2012. She has been studying the Master degree of Department of Chemical engineering from Faculty of Engineering, Chulalongkorn University.



## LIST OF PUBLICATION

Somrudee Chatchawanrat and Bunjerd Jongsomjit, “Catalytic behavior of carbon-based acid catalysts for the dehydration of ethanol.” The 3<sup>rd</sup> TIChE International Conference 2013, Department of Chemical Engineering, Faculty of Engineering, Khon Kaen University, Thailand, 17-18 October 2013.

